

1. Report No. SM-K1-04181	2. Government Accession No.	3. Recipient's Catalog No.
4. Title and Subtitle ACTIVE MICROWAVE SOIL MOISTURE RESEARCH	5. Report Date September, 1985	6. Performing Organization Code RSL/Radiation Lab
	7. Author(s) M. C. Dobson and F. T. Ulaby	8. Performing Organization Report No.
9. Performing Organization Name and Address Radiation Laboratory 4072 East Engineering Building The University of Michigan Ann Arbor, MI 48109	10. Work Unit No.	11. Contract or Grant No. NAG 5-30
	12. Sponsoring Agency Name and Address NASA/Goddard Space Flight Center Greenbelt, MD 20771	13. Type of Report and Period Covered Final Report
	5. Supplementary Notes	14. Sponsoring Agency Code
	NAG 5-30-1 = RL-2020	

6. Abstract

This paper summarizes the progress achieved in the active microwave remote sensing of soil moisture during the four years of the AgRISTARS program. Within that time period, from about 1980 to 1984, significant progress was made toward understanding (1) the fundamental dielectric properties of moist soils, (2) the influence of surface boundary conditions, and (3) the effects of intervening vegetation canopies. In addition, several simulation and image-analysis studies have identified potentially powerful approaches to implementing empirical results over large areas on a repetitive basis. This paper briefly describes the results of laboratory, truck-based, airborne, and orbital experimentation and observations.

7. Key Words (Suggested by Author(s)) Remote Sensing Soil Moisture Hydrology Radar Microwaves	18. Distribution Statement		
9. Security Classif. (of this report) Unclassified	20. Security Classif. (of this page) Unclassified	21. No. of Pages 58	22. Price*

*For sale by the National Technical Information Service, Springfield, Virginia 22161

TABLE OF CONTENTS

	<u>Page</u>
LIST OF FIGURES	i
ABSTRACT	1
1.0 INTRODUCTION	2
2.0 SOIL DIELECTRIC PROPERTIES	4
3.0 NON-VEGETATED SOIL	9
3.1 Soil Properties	10
3.2 Boundary Conditions	18
4.0 VETETATED SOIL	34
4.1 Bulk Canopy Biophysical Properties	35
4.2 Canopy Structure	44
5.0 SOIL MOISTURE RETRIEVAL	48
6.0 CONCLUSIONS	53
REFERENCES	55

LIST OF FIGURES

- Figure 1. Measured (a) real part and (b) imaginary part of the dielectric constant as a function of frequency with volumetric wetness as a parameter.
- Figure 2. Power reflection coefficient at nadir at 1.4 GHz versus (a) true volumetric soil moisture M_v and (b) percent of field capacity M_f .
- Figure 3. Angular pattern of retrieved true σ° for five soil surfaces with different roughness scales (σ from 1.1 to 4.6 cm) at (a) 1.5 GHz, (b) 4.25 GHz, and (c) 7.25 GHz (from [12]).
- Figure 4. Scattering coefficient dependence on RMS height and angle of incidence at (a) 1.1 GHz, (b) 4.25 GHz, and (c) 7.25 GHz.
- Figure 5. Computed normalized backscattering using the scalar approximation as a function of (a) incidence angle and (b) $k\sigma$.
- Figure 6. Computed normalized backscattering using the stationary-phase approximation (geometric-optics model) as a function of incidence angle and RMS slope.
- Figure 7. Scatterometer time response measured for a wheat-stubble field whose row pattern is shown in the insert. The observation angle was 20° .
- Figure 8. Comparison of canopy attenuation for various crops at (a) 2.7 GHz and (b) 5.1 GHz.
- Figure 9. (a) Linear regression of σ° (dB) versus M_f for bare fields, vegetation-covered fields, and both types combined; (b) variation of canopy backscattering coefficient with soil-moisture content for bare soil and individual crop types.
- Figure 10. Effect of a mature corn canopy undergoing progressive stages of defoliation on (a) emission and (b) backscattering at C-band.
- Figure 11. Cumulative percent area of all moisture-dependent pixels (excludes cultural features, water, and woodland) in each subregion as a function of absolute moisture classification error for (a) 100 m x 100 m radar resolution and (b) 1 km x 1 km radar resolution. M_f represents the true moisture and \hat{M}_f the moisture estimated by the radar (from [42]).

ACTIVE MICROWAVE SOIL MOISTURE RESEARCH

M. C. Dobson and F. T. Ulaby

Radiation Laboratory

Electrical Engineering and Computer Science

University of Michigan

Ann Arbor, MI 48109

Abstract

This paper summarizes the progress achieved in the active microwave remote sensing of soil moisture during the four years of the AgRISTARS program. Within that time period, from about 1980 to 1984, significant progress was made toward understanding (1) the fundamental dielectric properties of moist soils, (2) the influence of surface boundary conditions, and (3) the effects of intervening vegetation canopies. In addition, several simulation and image-analysis studies have identified potentially powerful approaches to implementing empirical results over large areas on a repetitive basis. This paper briefly describes the results of laboratory, truck-based, airborne, and orbital experimentation and observations.

1.0 INTRODUCTION

The objective of the AgRISTARS soil moisture project was to develop and evaluate the technology to make both remote and ground measurements of soil moisture. The attainment of this objective was viewed as a precursor to using soil-moisture information in application models for predicting crop yield, plant stress, and watershed runoff. This paper summarizes the advances made during the AgRISTARS program with respect to the sensing of soil moisture using active microwave techniques; a companion paper in this issue deals with passive microwave techniques [1].

Prior to the AgRISTARS program, the capability of active microwave techniques to sense near-surface soil moisture had been, for some years, an area of considerable research interest. A number of field experiments had been conducted, most of which used truck-mounted FM-CW scatterometers. The systems had been used as spectrometers over the 1 GHz to 18 GHz frequency band in order to investigate the spectral properties of radar response to first-order soil properties such as soil moisture and to the random component of soil roughness induced by agricultural tillage practices [2]-[4]. These efforts identified radar sensitivity to near-surface soil moisture as a function of surface roughness and soil texture for various combinations of the radar sensor parameters of frequency, polarization, and angle of incidence with respect to nadir [5], [6]. In general, the studies concentrated on non-vegetated soil surfaces and

approached the problem from an analytical viewpoint, i.e., as an optimization problem, with the objective of identifying sensor parameters having maximal sensitivity to and correlation with near-surface soil moisture but also having minimal sensitivity to surface roughness and agricultural canopy cover. The resulting recommendations for a C-band radar (at about 5 GHz) operating at angles of incidence in the 10° to 20° range have not been substantively altered by the findings of subsequent investigations.

Research undertaken as part of the AgRISTARS program was directed at verifying these preliminary findings and extending them via a parametric analysis of each of the scene variables expected to affect the radar backscattering from an agricultural setting. The scene variables examined include soil-moisture profile and sampling depth, soil bulk density, soil surface boundary conditions (such as random surface roughness, row direction effects related to ridge/furrow tillage practices, and local slope as related to local angle of incidence), vegetation canopies, and geographic conditions (such as variability in local topography, soil texture, field size and shape, and the presence of non-agricultural features such as urban areas, forests, and water bodies). The preceding variables were examined (sometimes not definitively) through a series of laboratory and field experiments generally coupled with concurrent modeling efforts. A summary of the significant results of these investigations is presented in the ensuing sections.

2.0 SOIL DIELECTRIC PROPERTIES

The dielectric properties of moist soils are quintessential in determining the microwave scattering and absorption by a soil medium. Whereas the relative permittivity of dry soil constituents is typically about 3 and depends upon packing density, the permittivity of water is about 80. Although naturally occurring soils are spatially and temporally complex media, it has proved convenient to examine the dielectric behavior of relatively simple and "homogeneous" test soils in the laboratory. This simplification is justified when applying soil dielectric properties to scattering and emission models at the microscale level; it breaks down at larger scales (related to sensor resolution) only because the true variance in the spatial and temporal properties is exceedingly difficult to quantify.

In general, a soil medium can be treated as a volume consisting of variable fractions of soil solids, aqueous fluids, and air. Soil solids are characterized by the distribution of particle sizes (texture) and the mineralogy of their constituent particles (particularly the clay fraction). Several laboratory studies have been conducted to investigate the effects of soil moisture, bulk density, and soil texture on the net dielectric behavior of the soil medium using either guided-wave or free-space transmission techniques [7]-[9]. In particular, these studies sought to quantify the role of dielectrically bound water (not necessarily chemically bound water), whose quantity is strongly dependent upon soil texture and mineralogy. The results both of the studies and of subsequent analyses [10] indicate that

- 1) the dielectric constant of dry soil is independent of frequency over the microwave region and is primarily dependent upon soil bulk density,
- 2) the addition of water to a dry soil medium results in an increase in the dielectric constant that is smaller in magnitude for initial increments of "bound water" than for subsequent additions of "bulk water,"
- 3) the quantity of "bound water" is controlled by soil texture and mineralogy (being roughly proportional to the soil clay fraction), which results in profound differences among soil types with respect to the dielectric constant at a given moisture content,
- 4) the observed differences among soil types are frequency dependent and are greatest at the lower frequencies (those less than approximately 3 GHz), where the effects of the effective salinity of soil fluids exert significant influence,
- 5) the frequency dependence of soil dielectric properties is generally of the Debye type and is similar in form to that observed for water, and
- 6) because the dielectric constant of moist soils is proportional to the number of water dipoles per unit volume, the preferred measure for soil moisture is volumetric.

The study by Wang and Schumugge [7] at 1.4 and 5 GHz resulted in an empirical formulation for the calculation of the soil dielectric constant as a function of soil moisture and soil texture. A later study by Dobson et al. [9] over the frequency range from 1 to 18 GHz resulted in both multifrequency empirical formulations and a physically based theoretical model that explicitly treats a number of soil physical properties including soil bulk density, specific surface area, cation exchange capacity, volumetric soil moisture, and the quantity and dielectric nature of "bound water." An example of the frequency response of soil dielectric properties is shown for silt in Fig. 1.

The scientific rationale for conducting the dielectric investigations was clearly twofold: first, to gain a fundamental understanding of the basic property governing microwave sensor response and, second, to provide an accurate data base for the derivation of dielectric properties as needed inputs to increasingly accurate and demanding microwave emission and scattering models. In parallel with the soil dielectric work, preliminary investigations have sought to determine the dielectric properties of common components of vegetation canopies such as fruit, stalks, and leaves [11]. These efforts have been complicated by the fact that the canopy elements are commonly similar to a wavelength in size, they assume preferred orientations in nature, and they may be irrevocably altered by the sample-preparation process.

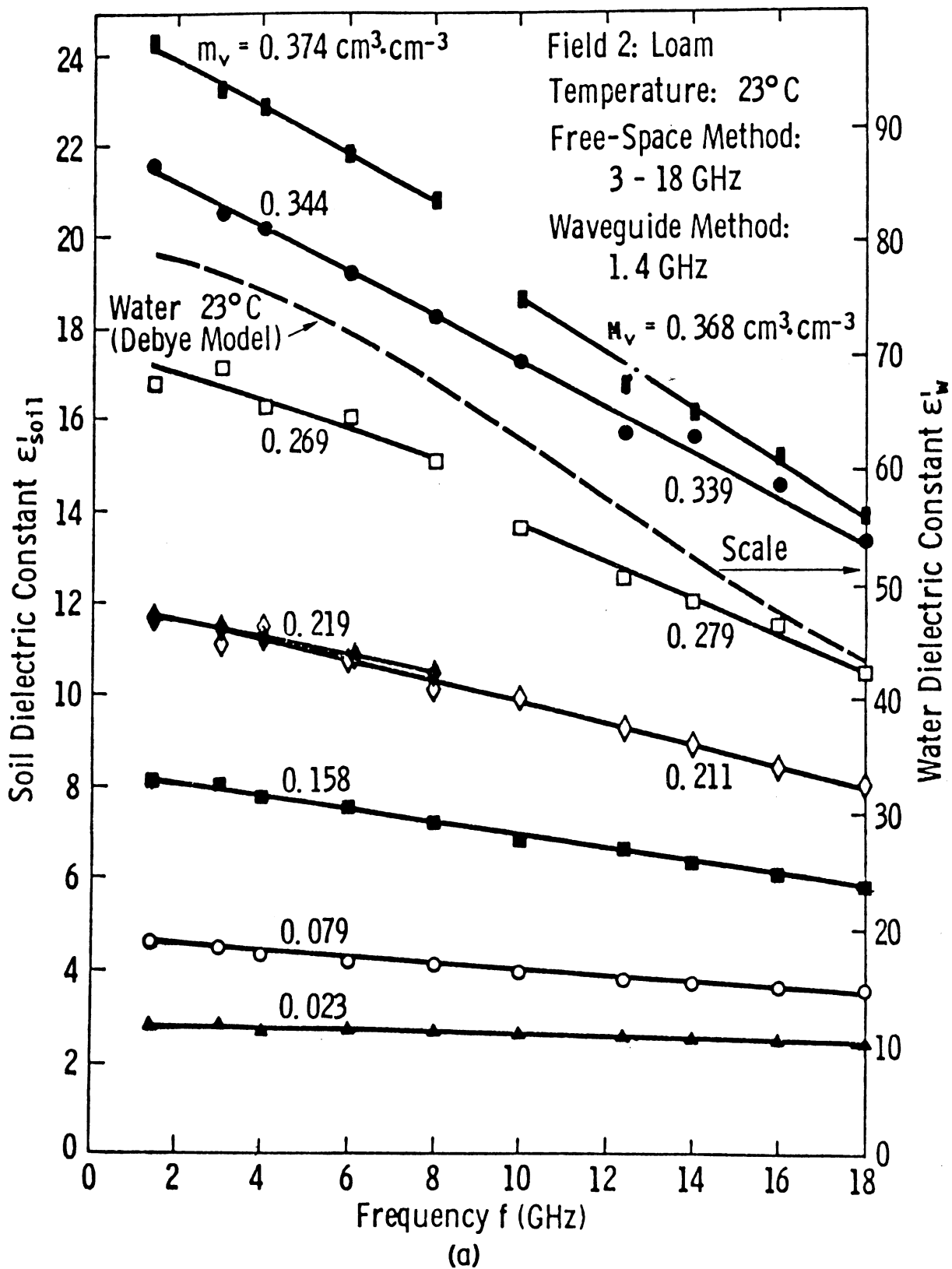


Figure 1a. Measured real part of the dielectric constant as a function of frequency with volumetric wetness as a parameter.

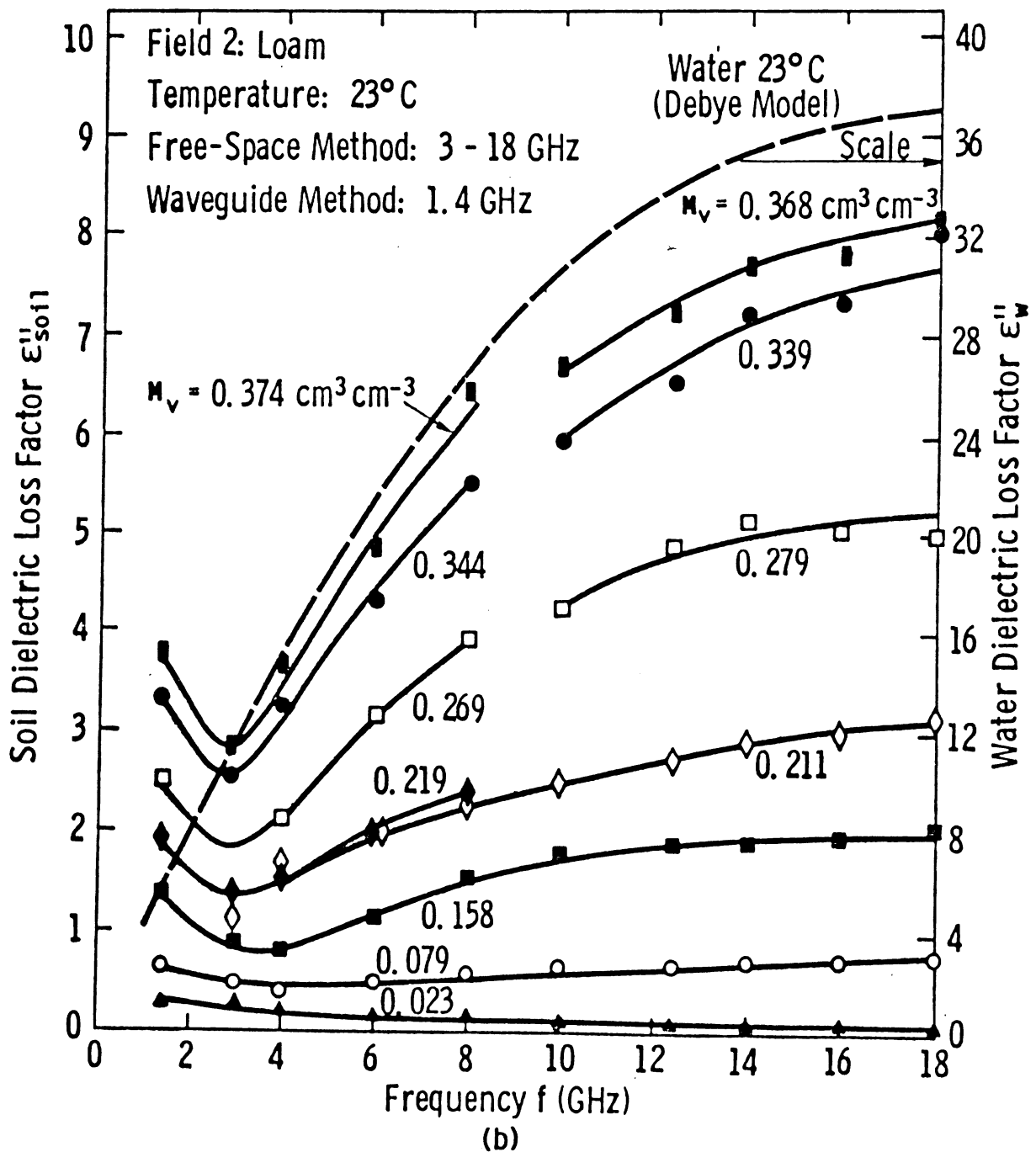


Figure 1b. Measured imaginary part of the dielectric constant as a function of frequency with volumetric wetness as a parameter.

3.0 NON-VEGETATED SOIL

The microwave energy incident upon the soil surface may be scattered, transmitted, or absorbed; the relative quantities of each of these processes and their directional characteristics are determined by the intrinsic dielectric properties of the soil medium and by the boundary conditions at the air-soil interface. Boundary conditions of interest include the small-scale random surface roughness generated by agricultural tillage practices, azimuthally dependent ridge/furrow patterns, and the slope of a terrain element, which affects the local angle of incidence.

A radar measures that quantity of the incident power which is backscattered, and, in the general case, this quantity can consist of both a coherent component (from specular reflection) and an incoherent component (from scattering). Although both terms are strongly dependent upon the Fresnel power reflection coefficient determined by the dielectric properties of the soil (as modified by surface roughness), the coherent component is more strongly dependent upon the angular properties of both the scene (roughness and local angle of incidence) and the sensor (beamwidth). Hence, the coherent component can dominate the integrated response at near-nadir angles, especially for systems having large beamwidths. For applications in which the purpose is to identify the backscattered signal that would be derived by an orbital synthetic-aperture radar (SAR) processed to have an effective pencil beam, the effective weighting by the antenna pattern of the measurement system (truck-mounted or airborne

scatterometer) must be taken into account. A procedure was implemented to retrieve the "true" backscattering coefficient from the truck-mounted scatterometer data, which was experimentally obtained at angles near nadir [12].

3.1 Soil Properties

Recent investigations have yielded considerable insight into the nature of the soil bulk properties that control the radar backscattering response. The studies have explored the role of soil moisture and profile shape, soil bulk density, and soil texture [5], [6], [13-16]. However, the effects of organic constituents, clay mineralogy, and stony soil inclusions remain largely unexplored.

Near-Surface Moisture Profile

For the simplest case, that of a semi-infinite, internally homogeneous soil layer bounded by a smooth surface, the power reflection coefficient at nadir is determined from the dielectric constant by

$$\Gamma = \left| \frac{\sqrt{\epsilon} - 1}{\sqrt{\epsilon} + 1} \right|^2 \quad (1)$$

where $\epsilon = \epsilon' - j\epsilon''$.

By applying Eq. 1 to dielectric data measured at 1.4 GHz for several different soil textures, Dobson et al. [10] found that values of Γ range between 0.04 for dry soil and 0.52 for saturated soil, which corresponds to a difference of 11 dB, as shown in Fig. 2. However, field experimentation with both truck-mounted and airborne scatterometers at this frequency exhibited a dynamic range of 12 to 15 dB over the same moisture range [5].

A comparison of scattering-model calculations with scatterometer-measured data from plots of smooth, bare soil led to the postulation of two possible explanations for the apparent discrepancy: (1) the existence of subsurface effects and (2) an impedance-matching layer at the surface. Allen et al. [17] discounted subsurface effects due to soil-moisture profile shape (i.e., increasing soil moisture versus depth for a dry surface layer) because these effects would typically lead to an increase in the reflection coefficient calculated for a dry surface. Assuming the existence of a transition zone (in which the upper millimeters of soil are considerably drier on a volumetric basis than the average of the top several centimeters) functioning as an impedance-matching layer, Allen et al. [17] compared field backscattering measurements to the solutions of a Kirchhoff scattering model using both Wilheit's [18] method for calculating the reflection coefficient from a layered medium and an iterative solution to the Riccati equation. This assumption yielded good fits to the measured data and indicated that the thickness of the transition layer is inversely related both to near-surface soil

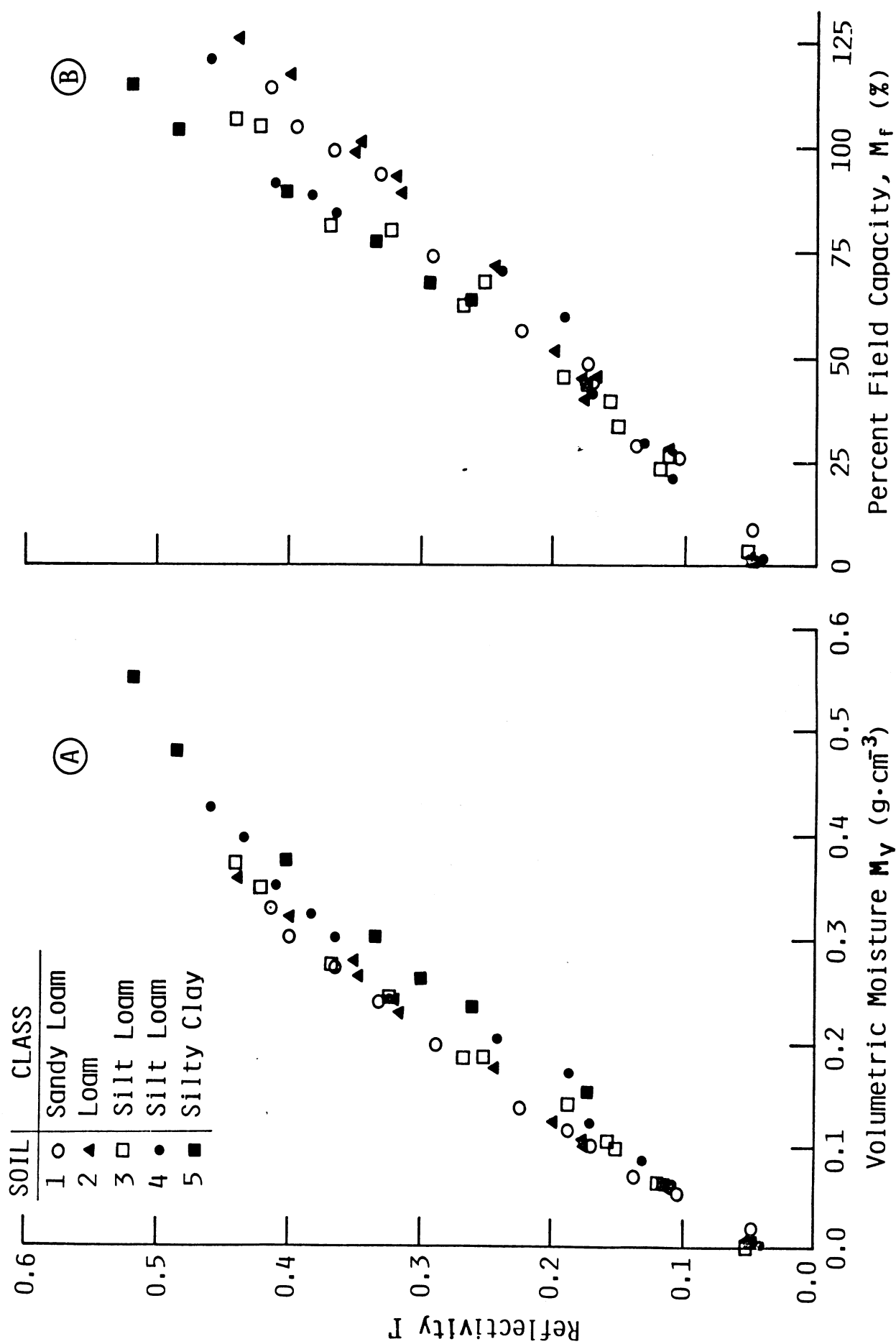


Figure 2. Power reflection coefficient at nadir at 1.4 GHz versus (a) true volumetric soil moisture M_v and (b) percent of field capacity M_f .

moisture and to frequency. From the standpoint of field measurements, this result emphasizes the need to pay critical attention to the moisture profile at the surface (at a sub-centimeter level) in order to produce exact model calculations of the backscattering from dry soils.

Soil Moisture Response

Before the advent of the AgRISTARS program, extensive measurement programs were conducted by the University of Kansas using truck-mounted scatterometer systems to observe test plots of non-vegetated soil with distinctive surface roughnesses and soil textures [2]-[5]. For a given soil condition (roughness or texture), radar backscattering was found to be linearly dependent upon the volumetric moisture M_V in the upper 2 to 5 cm of soil and to have linear correlation coefficients ρ typically on the order of 0.9,

$$\sigma^{\circ}(\text{dB}) = A + B M_V. \quad (2)$$

For a given sensor combination of frequency, polarization, and angle of incidence, the empirically derived regression coefficients A and B were found to be dependent upon soil surface roughness and soil texture, wherein A is primarily controlled by surface roughness, and B is primarily controlled by soil texture. For the prairie mollisols examined in these studies, polarization had no statistically discernible effect on the sensitivity term B.

Both combinations of like linear polarizations (HH and VV) yielded equivalent A, whereas cross-polarization produced a substantially lower value of A. In addition, the sensitivity term B was observed to be dependent upon both frequency and angle of incidence, gently decreasing with either increasing frequency or angle of incidence.

Subsequent studies by independent groups using ground-based scatterometers in the United States, France, and Japan [16], [19], [20] have verified many of these results. However, the results obtained by Hirose et al. [20] based on 9-GHz observations of Kanto loam represent a notable exception: they found that the cross-polarized sensitivity to near-surface volumetric soil moisture was four times that of the like-polarized backscattering. This result was attributed to the effects of multiple surface scattering; however, a similar effect has not been observed for very rough mollisols [5], [21].

Several investigators have reported the results of airborne scatterometer observations designed to sense soil moisture. These experiments were conducted during a series of overflights in 1978 and 1980 [21], [22]. Typically, these experiments used fan-beam Doppler scatterometers, operating at P-, L-, C-, and Ku-bands, mounted aboard a NASA/Johnson Space Center C-130 aircraft. Multitemporal observations of test areas in Kansas, Oklahoma, and Florida yielded fairly robust data sets in terms of soil moisture, vegetation cover, and surface roughness conditions. Analyses of these data support the conclusions reached on the basis of the more geographically limited truck-mounted scatterometer observations.

Calculations of the power reflection coefficient from the measured dielectric data shown in Fig. 2 indicate that the backscattering coefficient (in $m^2 m^{-2}$) should be linearly dependent upon soil moisture at moisture levels below saturation. Near saturation, the backscattering should level off, apparently becoming less sensitive to added increments of water. Because all of the field measurements of backscattering to date have reported σ° in dB, empirical regressions have taken the form given by Eq. 2. The scattering typically inherent in the field measurements makes it difficult to substantiate this expectation. However, field measurements have shown the saturation effect at high moisture contents, and these studies demonstrate that supersaturated and flooded soils behave as specular surfaces, which yield lower backscattering at off-nadir angles than non-saturated (but wet) soils [6], [23].

Soil Bulk Density

The dielectric studies of moist soils show that, for a given gravimetric soil moisture (the ratio of water mass to dry soil mass), the effect of increased soil bulk density should be to increase the reflection coefficient due both to increased soil solids and to water dipoles per unit volume of soil. Because the contribution of the dry soil solids is small relative to that of the water component, the effects of density on dielectric properties (and hence on the reflection coefficient) are largely accounted for by expressing soil moisture on a volumetric basis

(the ratio of water volume to moist-soil volume). The significance of soil bulk density effects has proved to be very difficult to verify by field measurements, due to (1) spatial variance in bulk density, (2) the temporal dynamics of bulk density, particularly for certain clay-rich soils, and (3) the great difficulty in obtaining an accurate determination of field bulk density for very thin layers of near-surface soil. The issue of soil bulk density effects has been addressed recently by several studies [10], [15], which conclude that very careful attempts should be made to quantify soil bulk density in the field in order to avoid mistaking the density effects on sensor response for soil textural or roughness effects on sensor response.

Soil Texture

Because most of the ground- and aircraft-based scatterometer studies of moist soils were purposely chosen to cover test sites having lateral homogeneity of soil type and texture, the effects of soil texture and mineralogy on radar backscattering are less well understood than properties such as surface roughness. The effects of soil texture are best inferred from dielectric studies and, as observed by Dobson and Ulaby [6], during truck-mounted scatterometer measurements.

The dielectric data strongly suggest that the first monolayer of water surrounding the surface of a soil particle is

largely irrotational under an impressed microwave field and hence is characterized by a relatively low dielectric constant that is dissimilar to either bulk water or ice [9]. The quantity of water that is dielectrically "bound" is determined by soil-particle size distribution (texture) and mineralogic composition via the specific surface area of the soil. The data also suggest that additional volumetric increments of water (beyond the "bound" component) exhibit dielectric properties that appear to be independent of soil texture per se but are dependent upon the effective salinity of the soil solution (which may be controlled by texture and mineralogy).

Attempts to compare early field investigations of different soils led to the development of a normalized soil-moisture index known as percent of field capacity, which is defined as the ratio of the gravimetric soil moisture to the moisture at a soil's field capacity. In practice, field capacity is typically defined on the basis of laboratory measurements of soil water retention at an arbitrarily defined value of 1/3-bar matric potential. This index was an attempt to account for the soil properties governing the apportionment of soil fluids into "bound" and "bulk" water. The application of this index to empirical comparisons of airborne radiometer [13] and truck-mounted scatterometer data [5] with soil moisture as observed for two different soil types yielded relationships that were apparently independent of soil type. Further work by Dobson and Ulaby [6] comparing the backscattering from three smooth soil surfaces having distinctive soil textures yielded the same result but also

showed that the expression of soil moisture in terms of matric potential produced linear relationships that were independent of soil texture. The linear relationship between matric potential and reflectivity [16] or backscattering [14] has also been noted by more recent investigations, which, unfortunately, have dealt with single soil textures only.

In partial contradiction to the preceding observations, an analysis of the dielectric data brings into question the physical basis of the percent-of-field-capacity index (and hence its geographical extensibility) on the basis that the index functions as a surrogate for accurate volumetric soil moisture information by partially accounting for the inter-soil variability in soil bulk density [10]. Hence, to some extent, the use of percent-of-field capacity may be useful, though not rigorously correct. As a consequence, it is believed that the best physical descriptor of soil moisture is volumetric, and the evidence to date indicates that the inter-soil variability in radar sensitivity to M_v is related to the soil-specific nature of the characteristic curve relating matric potential to M_v . However, this should be examined specifically by additional experimentation.

3.2 Boundary Conditions

The nature of the boundary at the air-soil interface determines both the amplitude and the phase properties of the reflection and transmission by the soil medium. The nature of the effects upon radar backscattering caused by soil surfaces can be subdivided into three categories:

- 1) effective local angle of incidence related to terrain slope,
- 2) small-scale surface roughness with laterally random size distributions, and
- 3) azimuthally dependent and generally periodic roughness patterns induced by agricultural tillage practices.

For a given sensor combination of frequency, polarization, and angle of incidence (relative to the mean surface), boundary conditions do not significantly affect the sensitivity to soil moisture but do add a bias term to the response.

Local Slope

The effects of a variable local angle of incidence can be inferred from an examination of Fig. 3, which shows the angular behavior of σ° for five non-vegetated soil surfaces as measured by a truck-mounted scatterometer. The angular dependence of the cross-polarized return is far less than that shown for like polarization. For a given frequency and polarization, the bias in σ° caused by the variation in local angle of incidence related to topographic relief is seen to be a function of angle of incidence, local slope, and the random roughness of the soil surface as seen in Fig. 4, whereby the smoother surfaces yield a greater bias per degree of angular uncertainty.

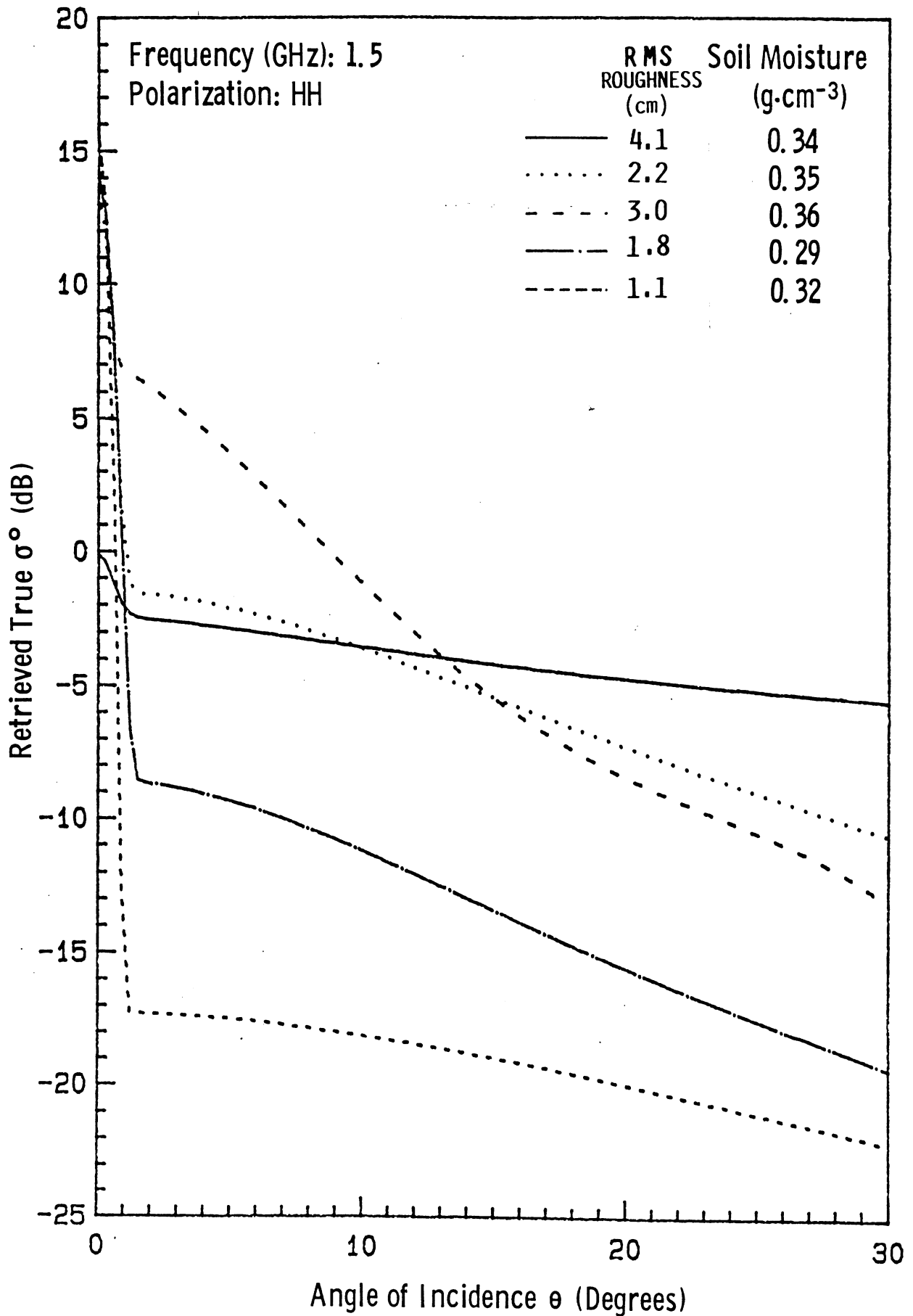


Figure 3a. Angular pattern of retrieved true σ^0 for five soil surfaces with different roughness scales (σ from 1.1 to 4.6 cm) at 1.5 GHz.

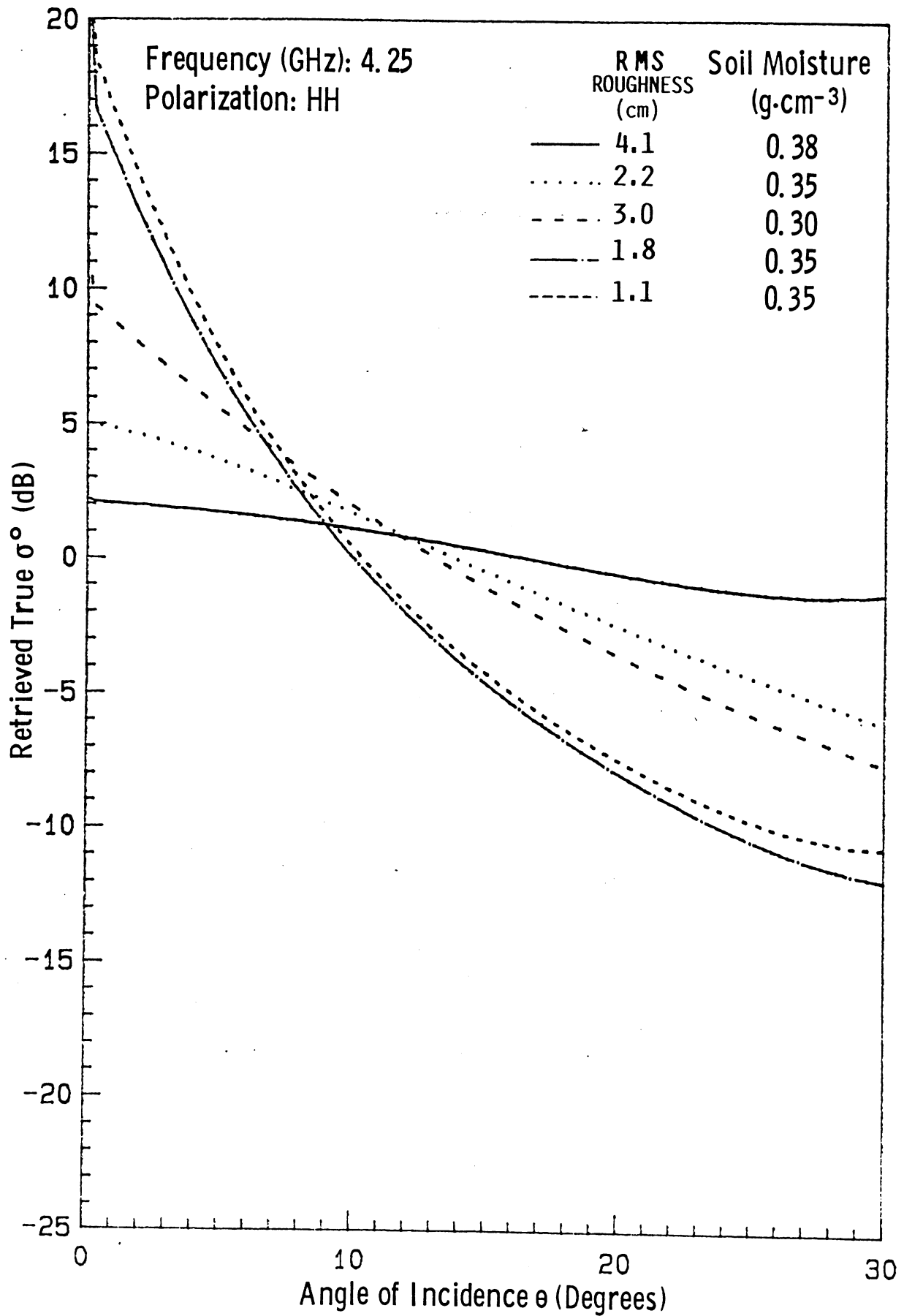


Figure 3b. Angular pattern of retrieved true σ^0 for five soil surfaces with different roughness scales (σ from 1.1 to 4.6 cm) at 4.25 GHz.

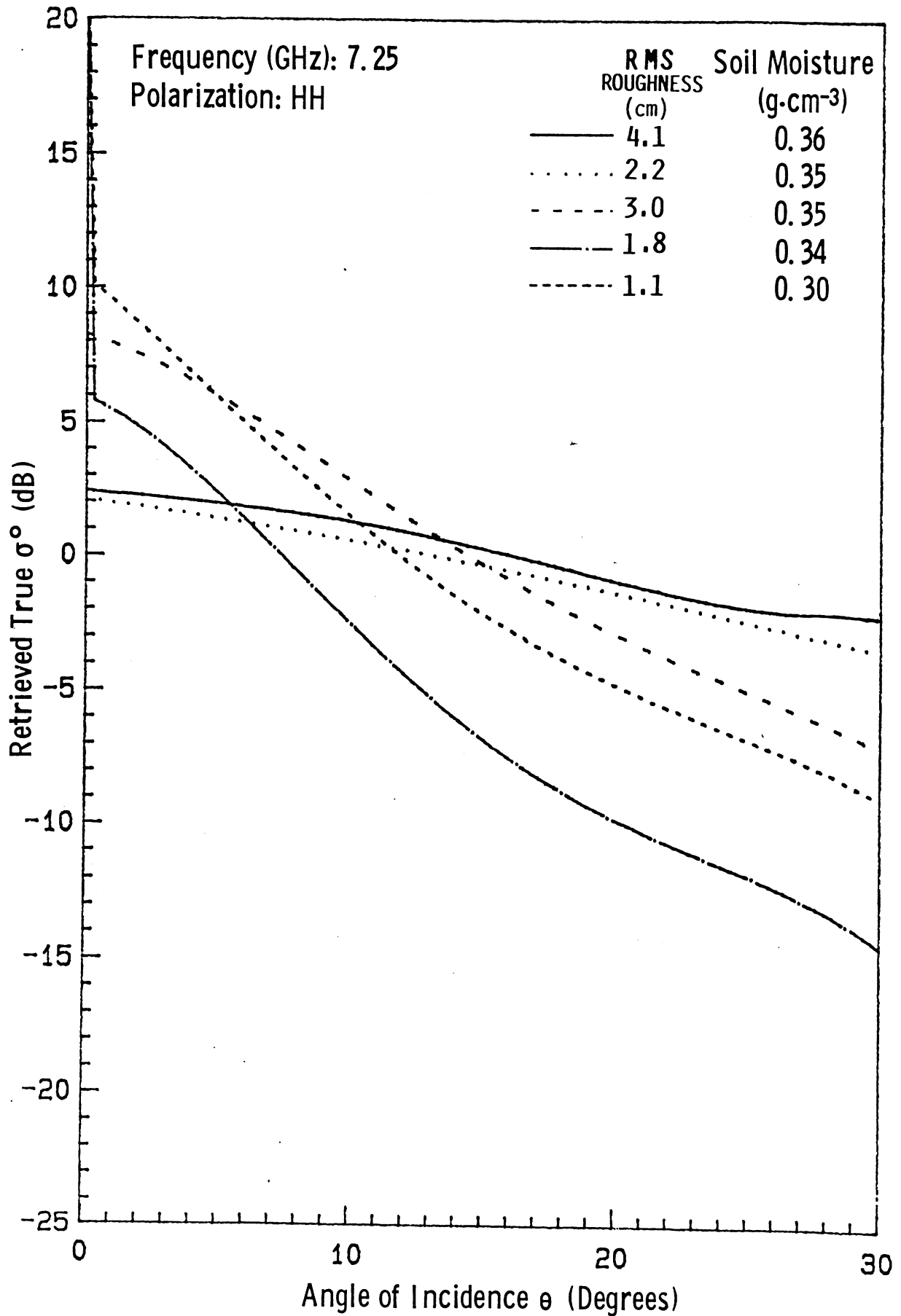


Figure 3c. Angular pattern of retrieved true σ^0 for five soil surfaces with different roughness scales (σ from 1.1 to 4.6 cm) at 7.25 GHz.

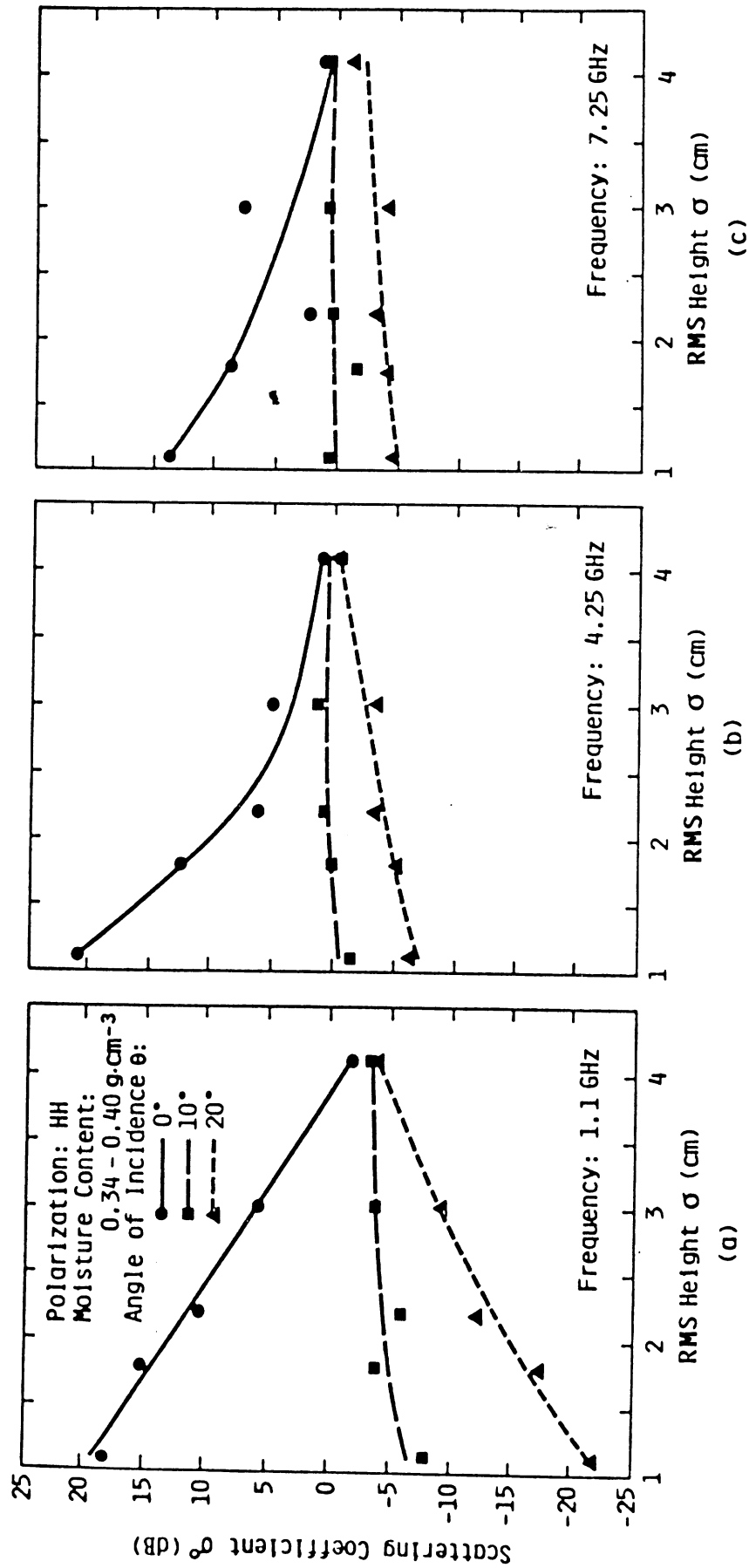


Figure 4. Scattering coefficient dependence on RMS height and angle of incidence at (a) 1.1 GHz, (b) 4.25 GHz, and (c) 7.25 GHz.

Random Surface Roughness

Examples of the measured effects of small-scale random surface roughness on radar backscattering are shown in Figs. 3 and 4 for non-vegetated soil surfaces that were specifically prepared for this purpose. The data used to derive Fig. 3 have been deconvolved to remove the coherent portion of the net measured backscattering related to the antenna pattern of the measurement system [12]. The angular effects of variable surface roughness are seen to decrease rapidly with frequency, as even the smoothest surface observed (RMS height = 1.1 cm) is no longer smooth by the Rayleigh criterion at frequencies above 3.4 GHz. The observed crossover in the angular responses for the various surfaces over the angular range from about 7 to 15° has been interpreted [5] as the optimal angular range for soil-moisture sensing with a minimal dependence on agronomically induced random surface roughness (certain geologic surfaces can be much rougher). Even within this angular range, however, it can be seen that roughness effects can be a significant source of error in soil-moisture determination from like-polarized backscattering for a particular field unless:

- 1) the roughness itself is concurrently extracted via multifrequency or multipolarized observation (like- and cross-polarized returns), or
- 2) soil moisture is estimated via a change-detection approach because surface roughness varies slowly with

time for agricultural fields in the absence of tillage operations.

The preceding approach seems to be tractable, because the backscattering behavior of randomly rough surfaces is shown to be well described by current scattering models. These models take two general forms with some modifications. The Kirchhoff model with the scalar approximation, or physical optics model [25], is used to describe the exponentially decaying angular dependence characteristic of smooth surfaces. The Kirchhoff model with the stationary-phase approximation, or geometric-optics model, is applied to relatively rough surfaces that display a slowly varying angular dependence near nadir.

The like-polarized backscattering coefficient of an isotropically rough surface consists of both a coherent term, σ°_{ppc} , which is important only at angles near normal incidence, and a noncoherent term σ°_{ppn} , which is important at all angles:

$$\sigma^{\circ}(\theta) = \sigma^{\circ}_{ppc}(\theta) + \sigma^{\circ}_{ppn}(\theta), \quad p = v \text{ or } h. \quad (3)$$

The coherent scattering coefficient is given by the approximate expression [24]

$$\sigma^{\circ}_{ppc}(\theta) \approx \frac{\Gamma_p(\theta)}{B^2} \exp(-4K^2\sigma^2) \exp(-\theta^2/B^2) \quad (4)$$

where

$$B^2 = (kR_0\beta)^{-2} + (\beta/2)^2,$$

$\Gamma_p(\theta)$ is the Fresnel reflectivity for polarization p at incidence angle θ , $k = 2\pi/\lambda$, σ is the surface rms heights, R_0 is the range from the antenna to the center of the illuminated area, and β is the one-sided beamwidth of the antenna for a non-imaging scatterometer or its pixel-equivalent for an imaging system.

For the noncoherent component, the physical optics model gives [25]

$$\begin{aligned} \sigma_{ppn}^{\circ}(\theta) &= 2 k^2 \cos^2\theta \Gamma_p(\theta) \exp[-(2k\sigma \cos \theta)^2] \\ &\cdot \sum_{n=1}^{\infty} [(4k^2 \sigma^2 \cos^2 \theta)^n/n!] \\ &\cdot \int_0^{\infty} \rho^n(\xi) J_0(2k \xi \sin\theta) \xi \, d\xi , \end{aligned} \tag{5}$$

where $J_0(\)$ is the zeroth-order Bessel function of the first kind, and $\rho(\xi)$ is the surface correlation function. Figure 5 shows plots of $\sigma_{ppn}^{\circ}(\theta)/\Gamma_p(\theta)$ as a function of θ and $k\sigma$ for an exponential surface correlation function $\rho(\xi) = e^{-\xi/L}$, where L is the correlation length of the surface. The geometric optics model gives the same expression for HH and VV polarizations [25]:

$$\sigma_n^{\circ}(\theta) = \frac{\Gamma(0) \exp(-\tan^2\theta/2m^2)}{2m^2 \cos^4\theta} \tag{6}$$

where m is the RMS slope and $\Gamma(0)$ is the Fresnel reflectivity evaluated at normal incidence. Plots of $\sigma_n^{\circ}(\theta)/\Gamma(0)$ versus θ are shown in Fig. 6.

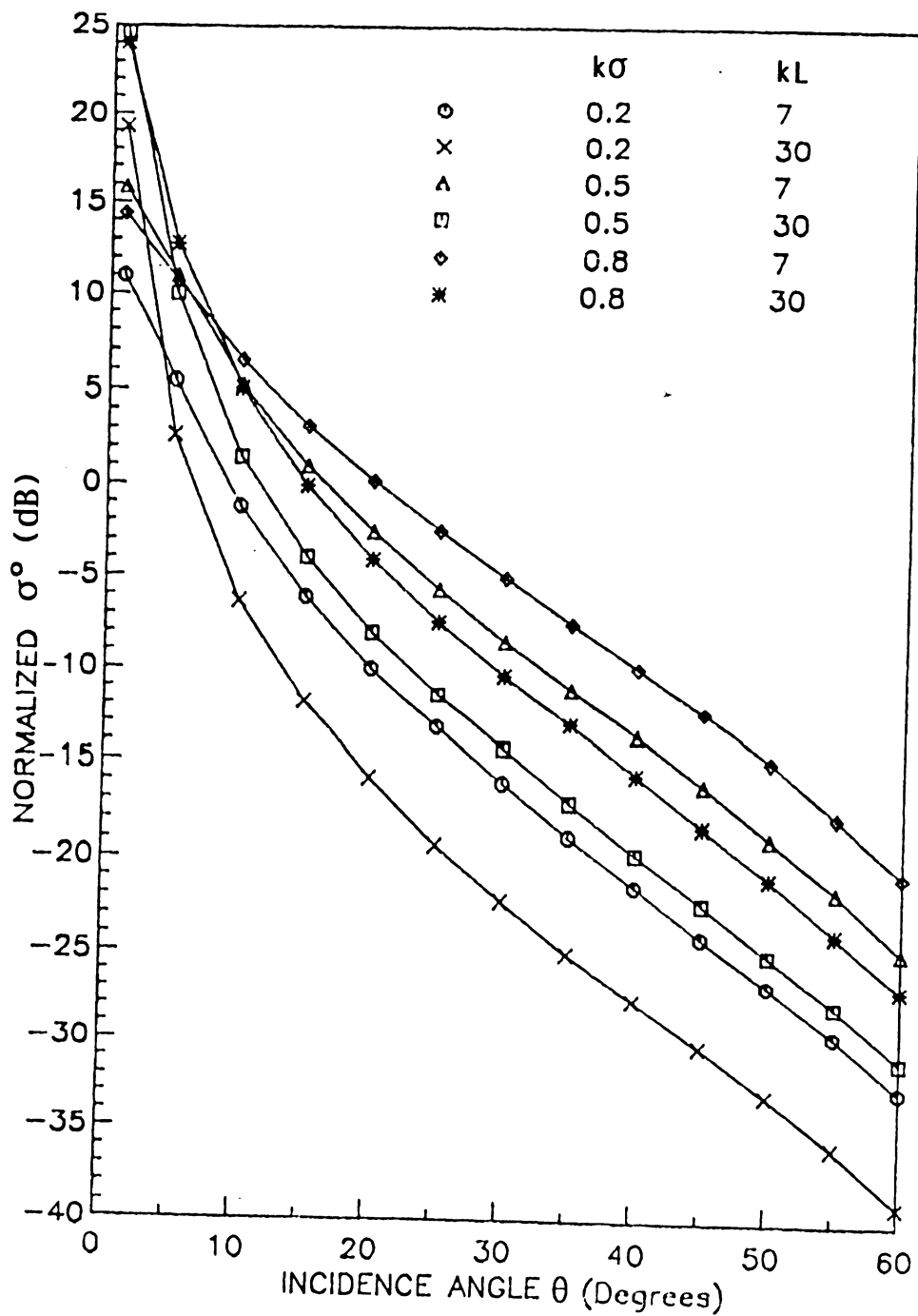


Figure 5a. Computed normalized backscattering using the scalar approximation as a function of incidence angle.

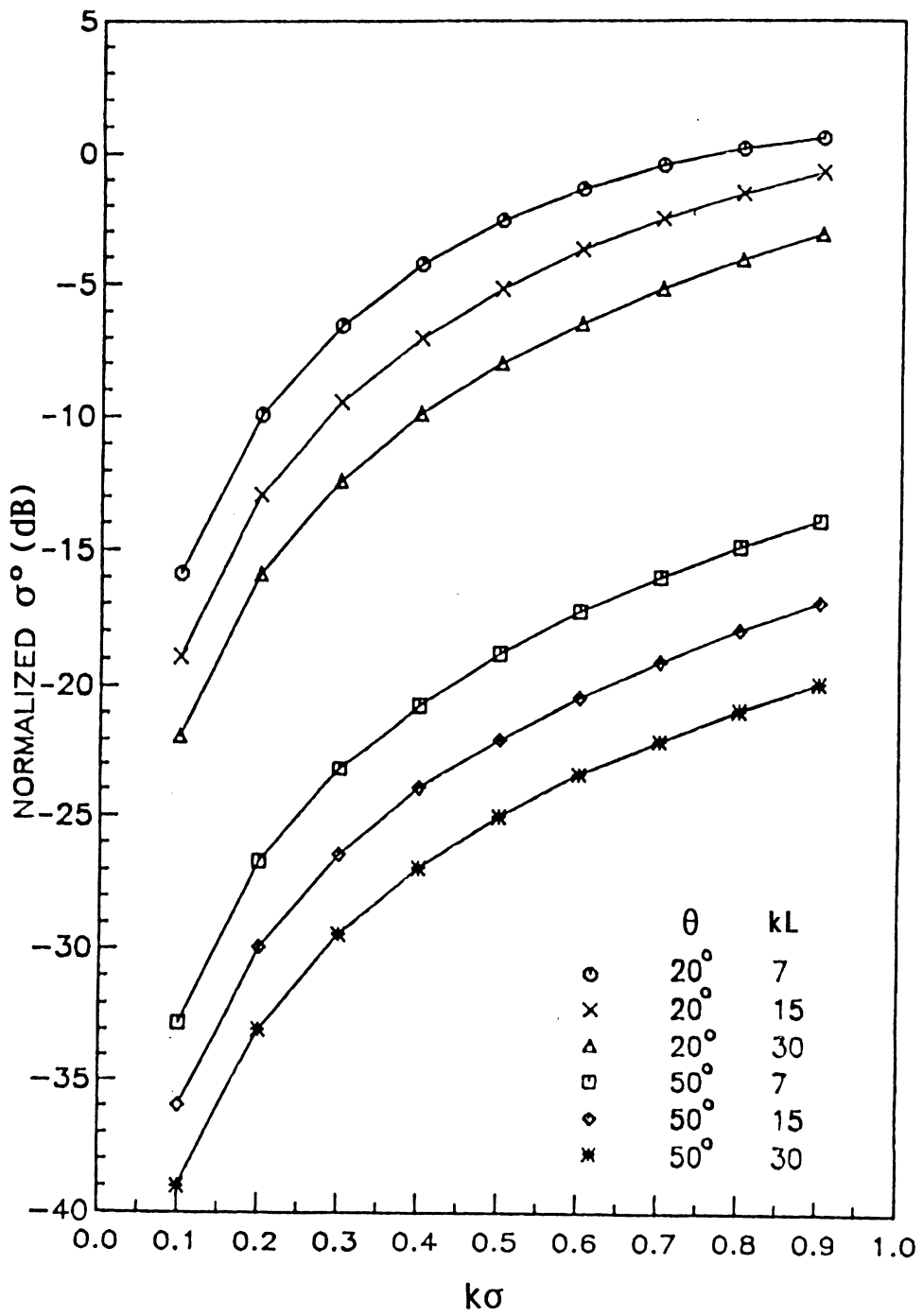


Figure 5b. Computed normalized backscattering using the scalar approximation as a function of $k\sigma$.

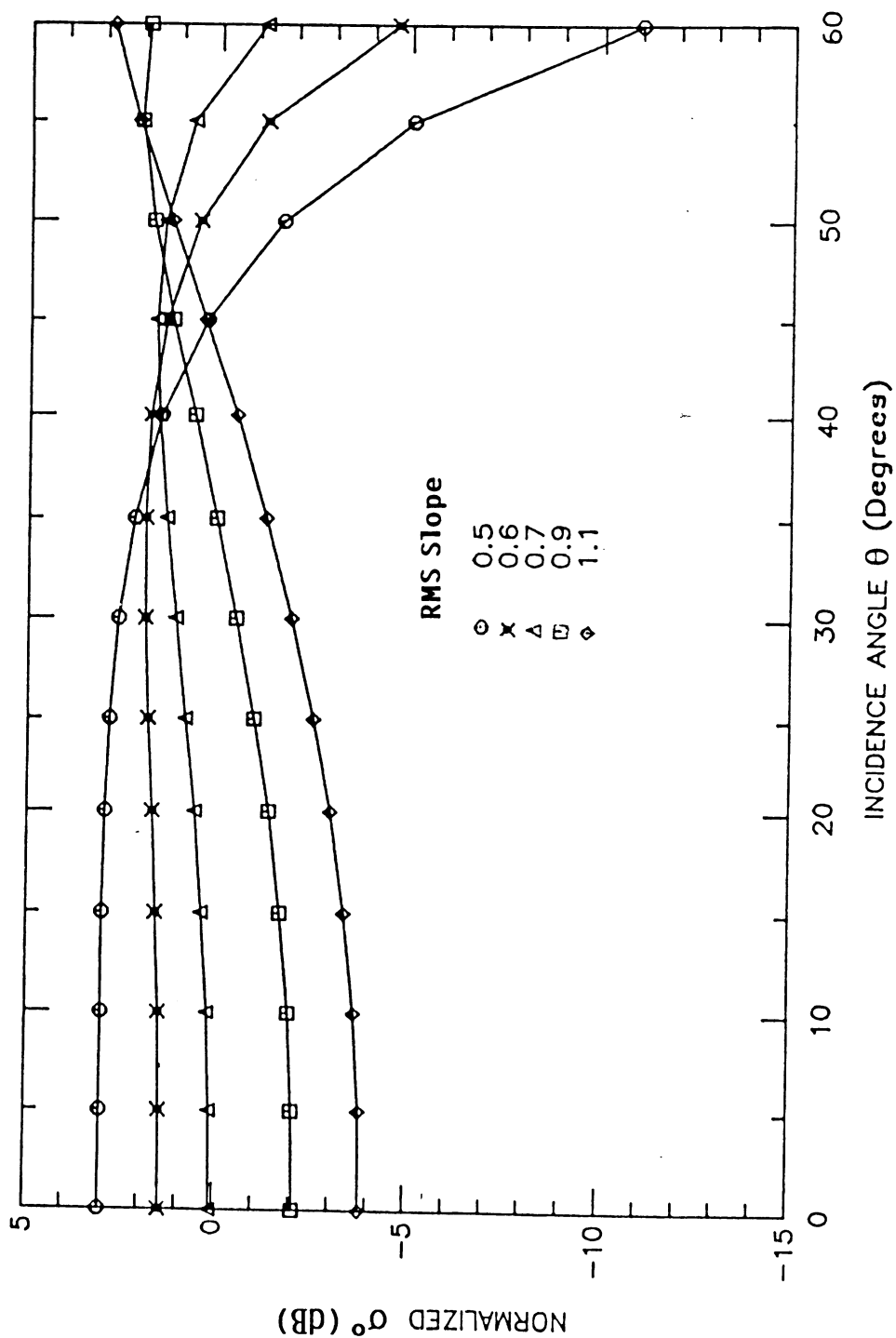


Figure 6. Computed normalized backscattering using the stationary-phase approximation (geometric-optics model) as a function of incidence angle and RMS slope.

Periodic Row Directional Effects

Agricultural crops are generally planted in parallel rows in either a rectangular format or in concentric rings (as in the case of some center-pivot irrigation systems). Soil tillage is also conducted by parallel operations using farm implements, which typically produce non-random and periodic ridge/furrow boundary conditions that modulate the small-scale and isotropic roughness components. The periodic components of surface roughness are of particular interest to the soil-moisture estimation problem because they have been observed to exert a considerable angular effect on radar backscattering [26]. Of major concern is the azimuthal dependence of the radar backscattering from ridge/furrow patterns. Examples of this type of dependence include the "bowtie" effect commonly seen on radar images of rectangularly tilled agricultural fields and in the airborne Doppler scatterometer time traces shown in Fig. 7. In certain respects, this phenomenon is analogous to the "cardinal direction" effect observed in radar images of urban scenes in which radar view angles orthogonal to cultural features yield very high levels of backscattering.

Observations of agricultural fields with truck-mounted and airborne scatterometers [21], [26], [27] and Seasat L-band SAR [28] suggest that radar is most sensitive to azimuthal viewing geometry for angles within 15° of orthogonal to the row direction and that this sensitivity decreases in an exponential fashion as view angle becomes parallel to row direction. Because many, but

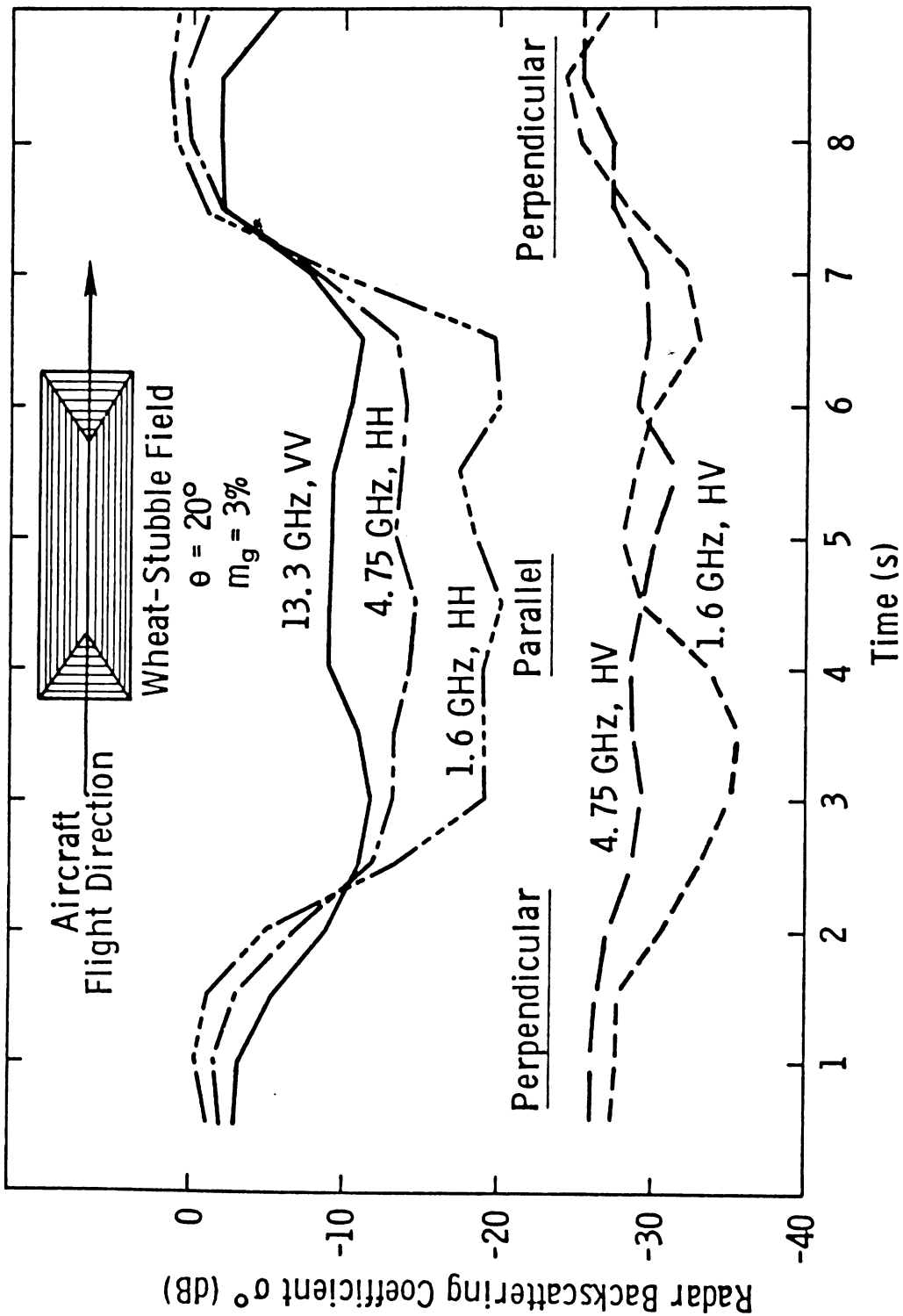


Figure 7. Scatterometer time response measured for a wheat-stubble field whose row pattern is shown in the insert. The observation angle was 20° .

not all, agronomically important areas are planted in a rectangular grid pattern with a North-South and East-West orientation, an operational orbital radar intended for soil moisture sensing should have an orbital inclination greater than 15° from polar orbit in order to minimize these effects at most latitudes.

Scatterometer observations have shown that the azimuthal effects of ridge/furrow patterns are also dependent upon the degree of isotropic small-scale surface roughness present, angle of incidence with respect to the ridge/furrow profile shape, frequency, and polarization. These effects are accurately described by a modified form of the scattering models previously introduced, which treats the periodic surface modulation as modifying the local angle of incidence for finite elements within the integrated illumination area [27]. In functional form, the backscattering coefficient $\sigma^\circ(\theta, \psi)$ of a periodic surface observed at an incidence angle θ (relative to the mean surface) and azimuth angle ψ (relative to the row direction) is related to $\sigma^\circ(\theta')$, the backscattering coefficient at the local angle of incidence θ' , by an integral of the form

$$\sigma^\circ(\theta, \psi) = \frac{1}{A} \iint_{\substack{\text{Illuminated} \\ \text{Area}}} \sigma^\circ(\theta') \, dA \quad (7)$$

where A is the illuminated area. The preceding form is given here simply to indicate that $\sigma^\circ(\theta, \psi)$ depends on the full angular range of $\sigma^\circ(\theta')$; the actual transformation involves the various

polarization states of $\sigma^\circ(\theta')$, which leads to a more complicated integral [27] than that given in Eq. 7. Many of the row-direction effects can be summarized using the look-direction modulation function $M(\theta)$ defined as the difference in σ° (dB) between parallel and perpendicular observations with respect to row direction as follows:

- 1) $M(\theta)$ is greatest for fields having the least random roughness and decreases rapidly as the surface becomes electromagnetically rough at a given frequency.
- 2) Related to the preceding, $M(\theta)$ decreases rapidly with increasing frequency.
- 3) $M(\theta)$ has a local maximum for local angles of incidence that are tangential to furrow slopes; this angle is typically in the 20 to 40° range and depends upon the field-specific tillage practices in use.
- 4) Importantly, the cross-polarized scattering coefficient is relatively insensitive to row direction effects and is typically found to be less than 2 dB for the reported measurements and models. The larger variance seen in the 1.6 GHz, HV response shown in Fig. 7 has been attributed to poor polarization-isolation of the antennas.

4.0 VEGETATED SOIL

Remotely sensing the moisture of the soil beneath a vegetation canopy has been the subject of keen interest and moderate experimental attention for the past 10 years. Early work, based largely on truck-mounted scatterometer measurements, sought to identify those sensor combinations of frequency and angle of incidence least sensitive to the presence of agricultural canopies. The studies concluded that the optimum parameters for moisture sensing should be frequencies of less than 6 GHz and angles of incidence of less than 20 degrees in order to minimize both the direct backscattering by the vegetation and the effective attenuation loss related to the two-way transmission through the canopy [29]. Subsequent studies using truck-mounted scatterometer data as well as data obtained by the airborne Doppler scatterometers have provided both simple empirical models and more robust theoretical models for the effects of agricultural canopies [30]-[32]. To date, most of the work has treated the vegetation canopy as an isotropic medium of disperse scattering elements with properties linked to bulk biophysical parameters such as crop-type and wet and dry biomass; some rigorous studies of the role of canopy structure (the size, shape, and orientation distributions of canopy elements) have been undertaken [33], but further work is needed.

4.1 Bulk Canopy Biophysical Properties

In general, the radar backscattering from a vegetated soil surface consists of three components: (1) a soil surface component, (2) a vegetation component, and (3) a surface-vegetation interaction component.

$$\sigma_{\text{total}}^{\circ} = \sigma_{\text{surface}}^{\circ} + \sigma_{\text{vegetation}}^{\circ} + \sigma_{\text{interaction}}^{\circ} \quad (8)$$

For an isotropic canopy characterized by an optical depth τ , the surface term is given by

$$\sigma_{\text{surface}}^{\circ}(k\sigma; kL; \epsilon; \theta; \psi, \tau) = T^2(\theta, \tau) \sigma_{\text{soil}}^{\circ}(k\sigma; kL; \epsilon; \theta; \psi; 0) \quad (9)$$

where $T(\theta, \tau)$ is the one-way transmissivity of the vegetation layer,

$$T(\theta, \tau) = \exp(-\tau \sec\theta). \quad (10)$$

The vegetation layer is treated as a uniform "cloud" of identical water particles, with the resulting scattering being entirely due to volume scattering, in which case there is no need to account for the scattering at the diffuse air-vegetation boundary. A full theoretical treatment of the vegetation term by Eom and Fung [32] permits multiple scattering within the vegetation layer. However, due to the small magnitude of the single-scattering albedo typically ascertained for crop canopies

at frequencies below 6 GHz (on the order of 0.1), empirical model evaluations have generally simplified the treatment of this term by considering only single scattering. This simplification results in the "cloud model" developed by Attema and Ulaby [30], which is only applicable to like-polarized returns:

$$\sigma_{\text{vegetation}}^{\circ} = \frac{3 \kappa_s \cos \theta}{4 \kappa_e} [1 - T^2(\theta, \tau)]. \quad (11)$$

where κ_s is the volume scattering coefficient, and κ_e is the extinction coefficient of the vegetation layer. A Rayleigh scattering phase function was assumed in the derivation leading to (11). Both parameters, which are dependent upon the biophysical properties of the canopy, are assumed to be polarization- and direction-independent. The surface-vegetation interaction term is determined by multiple reflection between the canopy and the surface, and its magnitude can be estimated approximately by

$$\sigma_{\text{interaction}} \approx \frac{3}{4} (1 + \cos^2 2\theta) \kappa_s T^2(\theta, \tau) \Gamma_p(\theta) \exp [-(2k\sigma \cos \theta)^2]. \quad (12)$$

This term is thought to become significant for sensor configurations for which the transmission loss is small and when there is significant scattering from either the vegetation volume or the soil surface. The surface-vegetation interaction term can be the dominant term in cross-polarized return.

Empirical evaluations of scatterometer data with respect to Eq. 8 have generally ignored the contribution of the interaction term and have sought to define the remaining model coefficients

based upon multifrequency or multiangle curve-fitting solutions for single-target observations [34] or have sought to define crop averages for the vegetation term and loss over a growing season [35]. Attempts to estimate the canopy loss factor on the basis of measurements of the dielectric properties of the vegetation have resulted in good fits to the measured data [11], [36]. In addition, several recent attempts have been made to define the loss parameter directly from one-way canopy transmission measurements using scatterometers at C- and X-bands [36], [37] and radiometers at S- and C-bands [38].

The one-way canopy loss as derived from radiometer observations of test plots of wheat, corn, and soybeans is shown in Fig. 8 as a function of crop-development stage. These values were obtained through a comparison of the apparent brightness temperatures of test plots in their natural state with those of adjacent plots in which the underlying soil surface was covered with a reflective material (wire mesh screens) or microwave absorber. Temporal behavior is clearly related to changes in vegetation biomass and to the appearance of distinctive canopy structural elements; the exact nature of these relationships remains to be determined. In general, the studies conducted to date show that

- 1) both the canopy loss and the vegetation volume scattering coefficient are linked to the canopy's biophysical properties, and especially, but not exclusively, to canopy type, canopy structure, and the water volume fraction within the canopy;

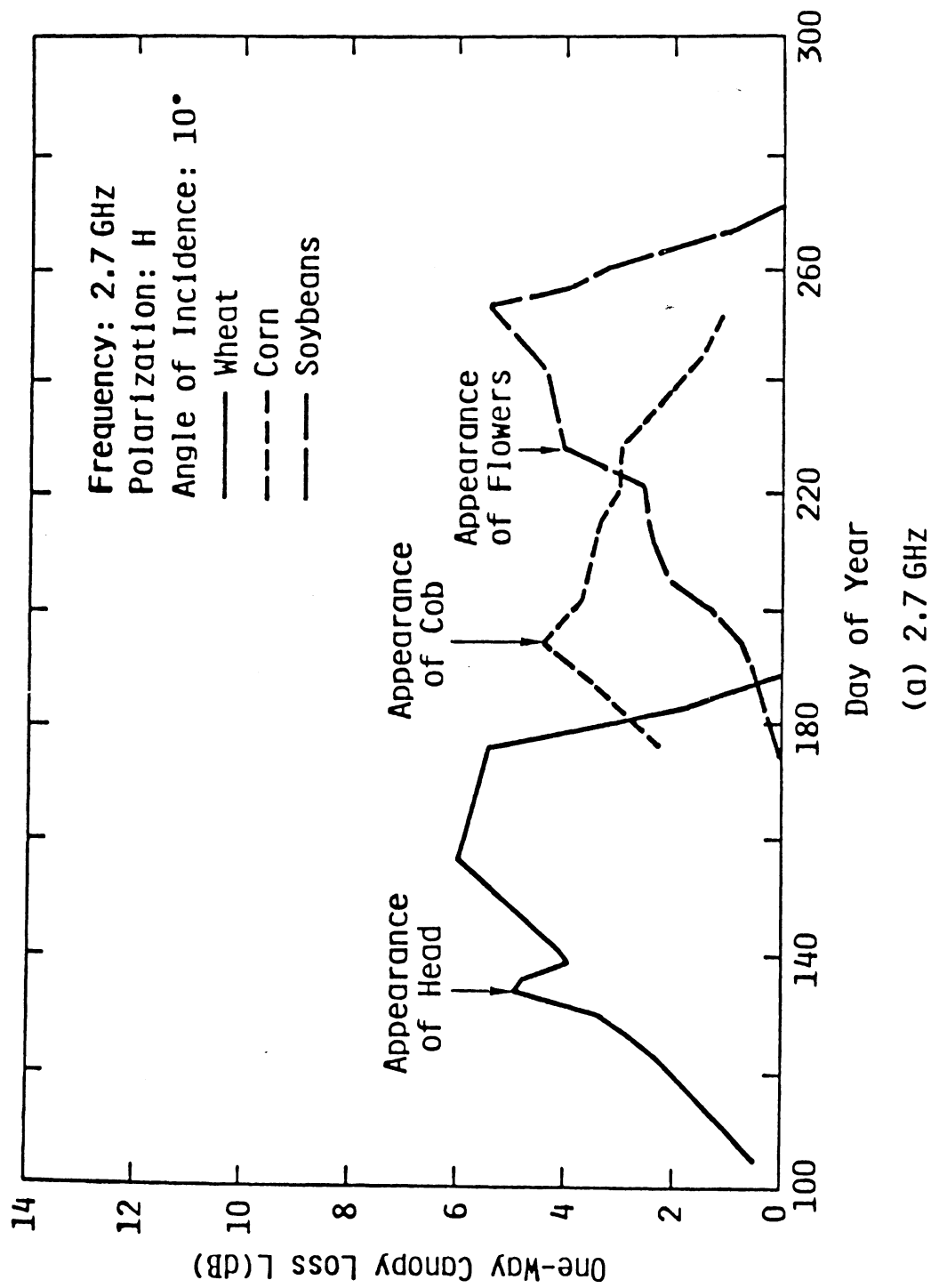


Figure 8a. Comparison of canopy attenuation for various crops at 2.7 GHz.

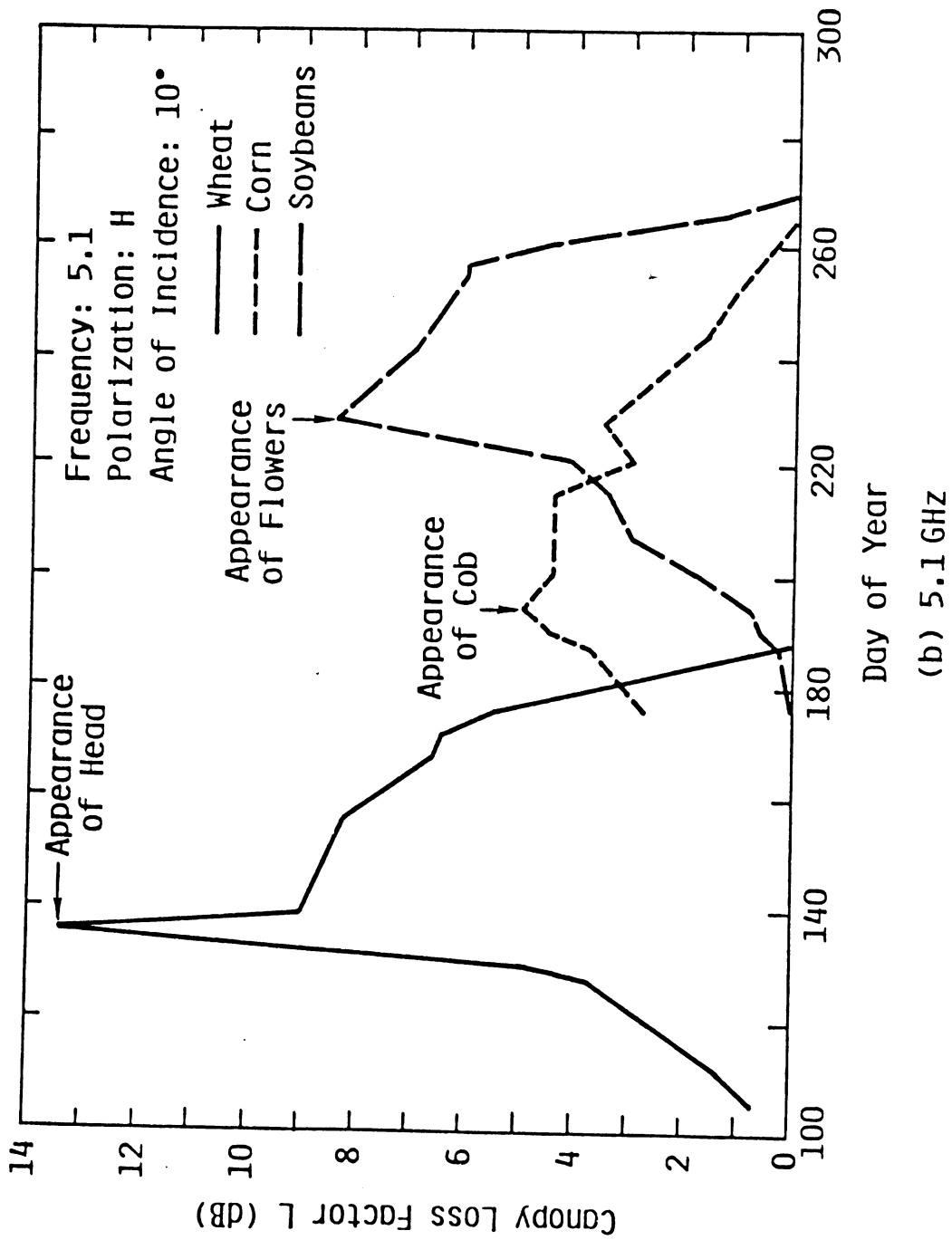


Figure 8b. Comparison of canopy attenuation for various crops at 5.1 GHz.

- 2) the canopy loss and the volume scattering coefficient increase with frequency;
- 3) the vegetation term in Eq. 8 tends to dominate the net return as either frequency or incidence-angle increases; and
- 4) the interaction term functions to enhance radar sensitivity to the moisture contained in the soil beneath a vegetation canopy.

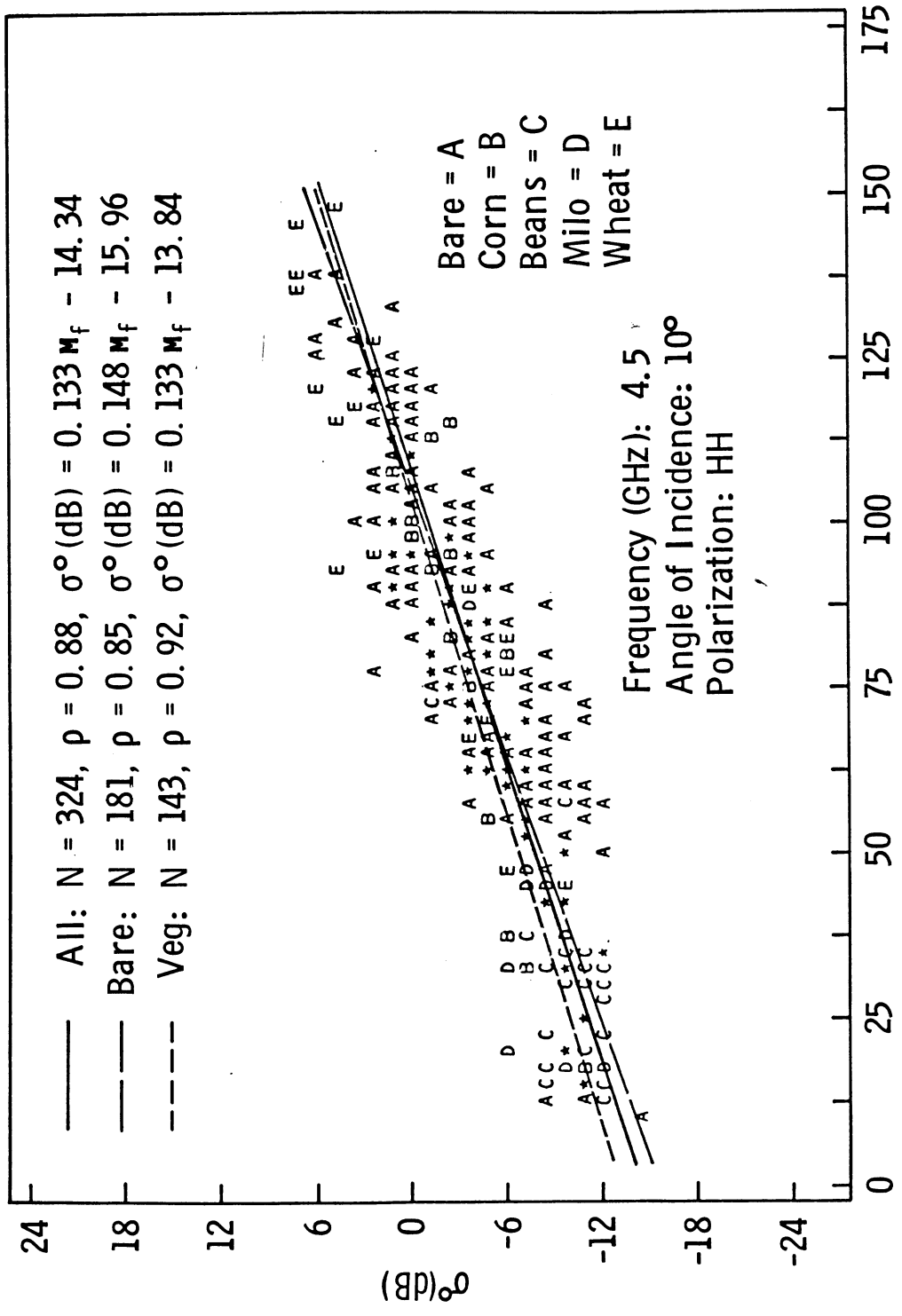
For purposes of soil-moisture sensing, it is preferable that the sensing system exhibit no sensitivity to canopy biophysical parameters. If this cannot be the case, it is pertinent to define how much the canopy's effects reduce radar sensitivity to near-surface soil moisture for canopy conditions typical of an agricultural setting. The effects of canopies of corn, soybeans, wheat, and milo (sorghum) on radar sensitivity to soil moisture at the sensor configuration deemed least sensitive to surface-boundary conditions (C-band at 10 to 20° angles of incidence) have been examined empirically using multiyear scatterometer observations [35]. Data obtained over the period from crop emergence to crop harvest were used to define average canopy loss and $\sigma^0_{\text{vegetation}}$ for each crop type through a linear regression approach that assumed σ^0_{soil} to be that calculated from measured soil moisture by

$$\sigma^0_{\text{soil}} = 0.025 \exp(0.034 M_f), \quad \text{m}^2\text{m}^{-2} \quad (13)$$

where M_f is the 0-5 cm percent of field capacity. Equation 13 results from the linear regression of 181 observations of bare soil plots with RMS surface-height variations ranging from 0.7 cm to 4.3 cm at C-band with HH polarization and a 10° angle of incidence; the linear correlation coefficient was found to be 0.85 [39]. Assuming a negligible interaction term (Eq. 12), the average canopy effects yield the responses shown in Fig. 9. It is apparent from Fig. 9 that at low soil-moisture levels (less than 50% of field capacity) the backscattering contribution from the crop canopy itself dominates the total return, whereas at higher moistures, the canopy loss causes a reduction in the net backscattering of between 0.7 dB and 2.0 dB for corn and milo, respectively, as compared to that from bare soil alone. Application of the regression procedure to all 143 observations of the various crops at this sensor combination yielded a general algorithm for estimating the moisture of soil beneath agricultural crop canopies with a linear correlation coefficient of 0.91 [39].

$$\begin{aligned}\sigma^\circ &= \sigma_v^\circ + T^2 \sigma_{\text{soil}}^\circ \\ &= 0.066 + 0.75 \sigma_{\text{soil}}^\circ, \quad \text{m}^2\text{m}^{-2}. \quad (14)\end{aligned}$$

In an analysis of the prediction errors arising from the use of generalized algorithms such as Eq. 13 for bare soil or Eq. 14 for vegetated soil, Ulaby et al. [35] concluded that it would be difficult to estimate soil moisture with any good degree of accuracy for low soil-moisture conditions (less than about 50% of field capacity) from a single sensor observation unless the



Soil Moisture Content in Top 5-cm Layer, M_f (% of Field Capacity)

Figure 9a. Linear regression of σ^o (dB) versus M_f for bare fields, vegetation-covered fields, and both types combined.

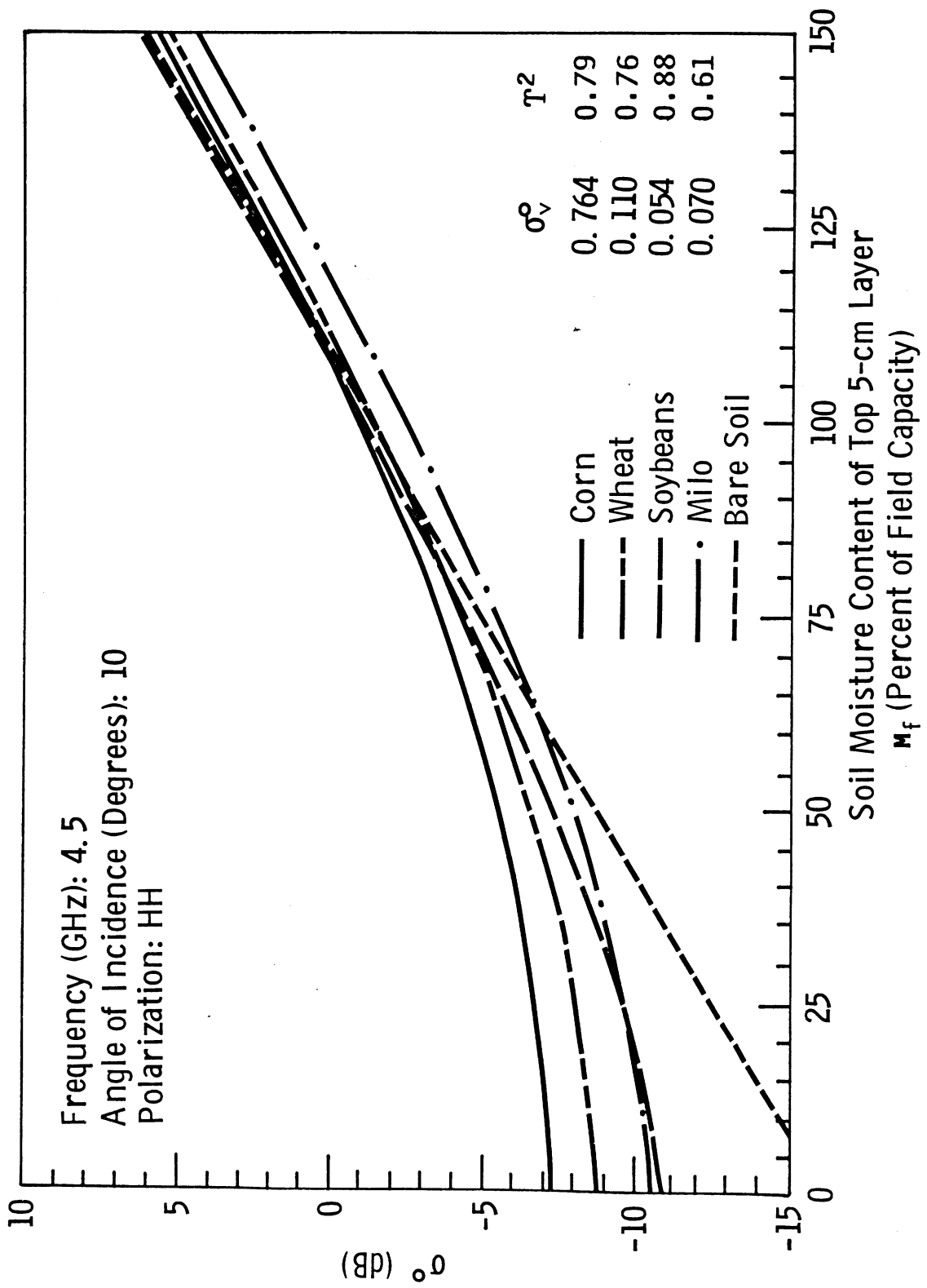


Figure 9b. Variation of canopy backscattering coefficient with soil-moisture content for bare soil and individual crop types.

presence of a canopy cover is known a priori or from other sensor observations (visible/IR or some other microwave frequency, polarization, or angle). On the other hand, for soil moisture conditions greater than 50% of field capacity, it is estimated that the 90% probability confidence interval would yield an uncertainty of $\pm 15\%$ of true field capacity, which corresponds to an uncertainty in volumetric moisture of about ± 0.02 and $0.05 \text{ cm}^3 \text{ cm}^{-3}$ for sands and silty clay soils, respectively. It is interesting to note that of the 583 discrete moisture observations made in Kansas between May and November, 80% had 0 to 5 cm moisture values in excess of 50% of field capacity.

4.2 Canopy Structure

The canopy structure is the complex spatial organization of discrete canopy components such as stalks, leaves, and fruit. Each component has a characteristic size, shape, orientation, and location distribution. In part because canopy structure is exceedingly difficult to quantify under natural field conditions, very few experiments have been conducted to examine its effects upon radar backscattering with respect to frequency, angle, and polarization. As a consequence, the impact of the variability of canopy structure upon radar sensitivity to soil moisture over time or between species cannot be specifically addressed. Nevertheless, several very interesting studies have been conducted and can be classed into two groups: transmission measurements [36], [37] and defoliation experiments.

The transmission measurements examined the vertical structure of wheat (grain heads versus stalks and leaves) with respect to polarization and local angle of incidence at X-band and demonstrated that in certain cases the layered structure of the canopy is important because canopies having strong angular properties (such as vertical stalks) can couple differentially at HH and VV polarizations [36] [37].

The defoliation experiments examined the backscattering and emission from canopies from which successive layers or types of canopy components had been progressively removed (by cutting). Figure 10 is an example of a corn canopy monitored with a scatterometer and a radiometer (both at 5.1 GHz) through successive defoliation stages until only the bare soil surface remained. For the radiometer, the canopy brightness temperature is dominated by the vegetation contribution at all angles; the increment in brightness temperature over that observed for the bare soil case is roughly proportional to the overlying water density of the canopy. In sharp contrast, the radar backscattering is observed to be insensitive to the presence of the corn canopy at incidence angles of less than 15° . At higher angles, the backscattering contribution of the canopy increases and is dominated by the return from the vertically aligned stalks and cobs, whereas the canopy loss component is apparently dominated by the leaves. Observations such as these strengthen the argument for using incidence angles near nadir for radar sensing of soil moisture.

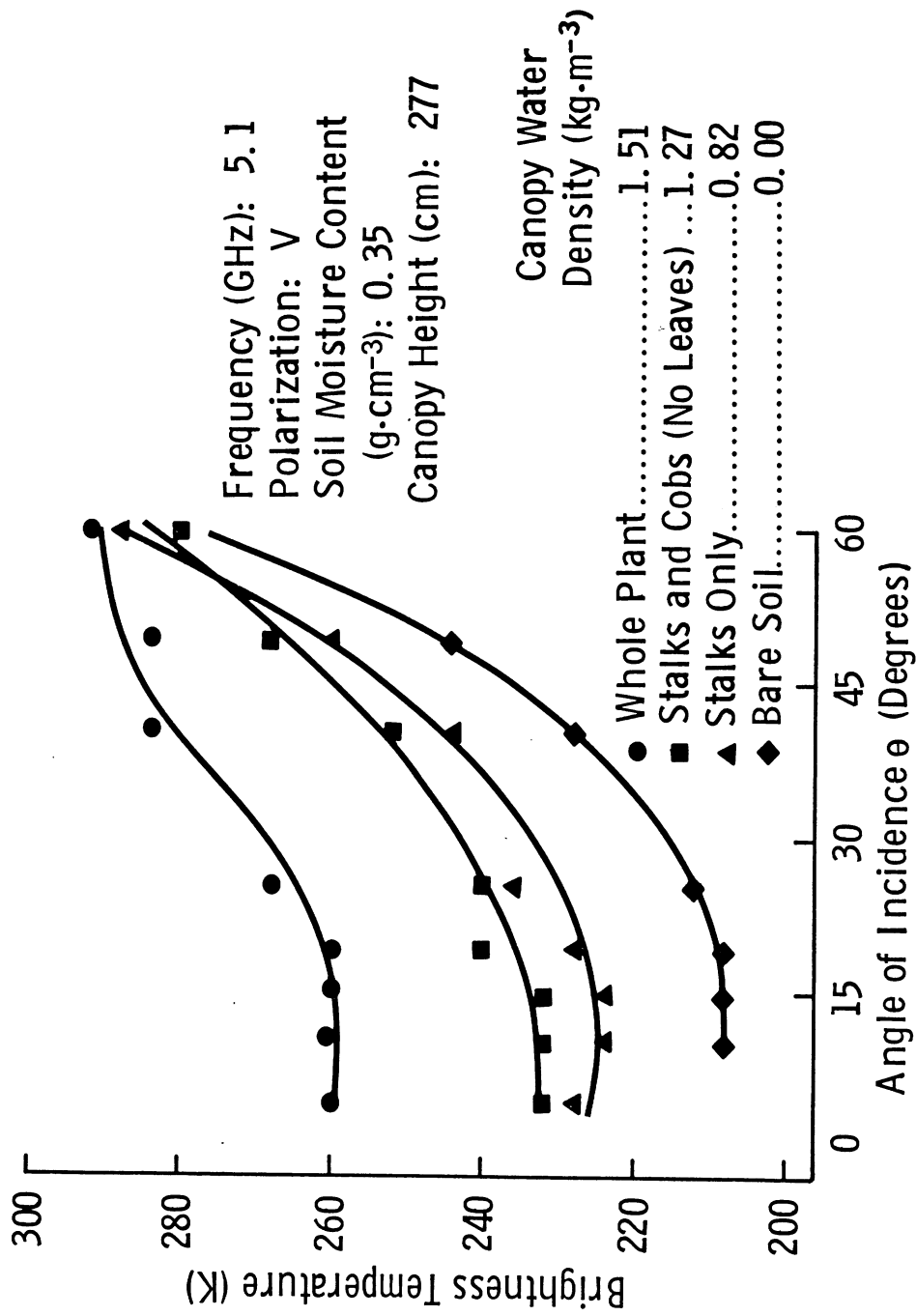


Figure 10a. Effect of a mature corn canopy undergoing progressive stages of defoliation on emission.

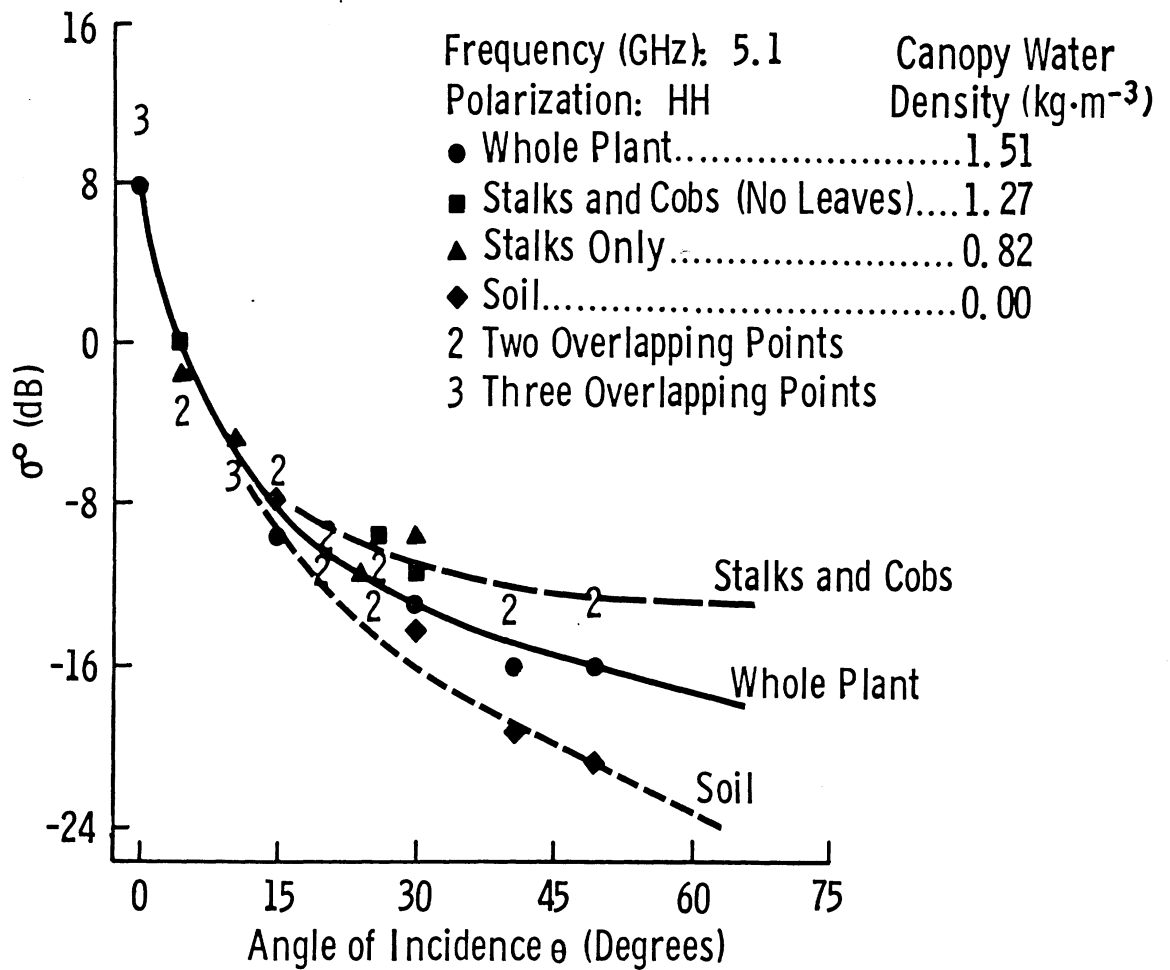


Figure 10b. Effect of a mature corn canopy undergoing progressive stages of defoliation on backscattering at C-band.

5.0 SOIL MOISTURE RETRIEVAL

The ultimate objective of the soil-moisture research conducted under the auspices of the AgRISTARS program is to develop the algorithms and methodology necessary for retrieving soil-moisture estimates on an areal basis for applications in hydrologic and agronomic monitoring and assessment. The sensitivity of radar backscattering to scene parameters including soil moisture, soil texture, soil density, surface roughness, surface slope, crop-canopy cover, and row-directional effects has been examined, either independently or in combination, by means of scatterometer studies of individual test plots in which the scatterometers were capable of relatively fine spatial resolution. The next logical step, then, in the analysis is to examine the combined effects of all scene variables on the capacity of radar to accurately estimate soil moisture for an imaging system with a coarser resolution, such as an orbital SAR.

Experimental work in this area has been limited to the L-band and HH-polarized SAR systems carried by Seasat in 1978 [28] and SIR-B in October of 1984. The data produced by the SIR-B mission are currently under investigation by several research groups. Although the scatterometer studies indicate that this frequency and polarization combination is less than satisfactory for purposes of soil-moisture sensing, primarily because of the pronounced dependence upon surface roughness and row-directional effects, the Seasat data were found to be highly correlated with near- surface soil moisture ($\rho = 0.84$) for

agricultural test field in the Great Plains for which concurrent ground truth was available [28]. In addition, a qualitative analysis of several Seasat scenes over Iowa revealed a dramatic sensor sensitivity to antecedent rainfall events, although corresponding ground truth was not available to resolve the question of whether the sensor response was driven by free water present on the crop canopies or by soil moisture (or both) [40].

Because orbital sensors with the scatterometer-defined optimal sensor configuration (i.e., C-band at 10° to 20° angles of incidence) are not yet available, the expected performance of such systems has been tested via simulation studies that incorporate all known sensor and scene characteristics [41-43]. These studies have sought to define both sensor characteristics (i.e., resolution, antenna size, power requirements, and data rate) and the influence of scene confusion factors (i.e., topographic effects, variable canopy cover, and the complex spatial distributions of water bodies, forests, and urbanized areas) on the accurate retrieval of soil moisture from a SAR image.

The simulation studies are based upon digital terrain models in which each terrain element is characterized as to land-cover category, soil properties, and crop row direction. Typically, meteorologic events are used to simulate dynamics in the near-surface soil-moisture distributions over the test region as a function of time and local evapotranspiration demands. At selected time intervals, the backscattering properties of each sub-resolution element are defined by a Monte Carlo procedure

based upon the scatterometer studies and estimates of "true" natural scene variability. The effects of signal scintillation (fading), shadowing, and layover are also incorporated into the image-formation model.

Early simulations of a 20 km x 20 km, largely agricultural test region indicated that 0 to 5 cm soil moisture (expressed as a percent of field capacity) could be retrieved with an accuracy of $\pm 20\%$ for 90% of the agricultural area using a C-band SAR with HH polarization at 7° to 17° angles of incidence and resolutions of 100 m x 100 m [41, 42]. The simple retrieval algorithm required only the range position of the image pixel and the magnitude of the backscattered signal as input. A subsequent simulation for a much larger area, ≈ 100 km x 120 km, which included more diverse topographic and land-cover conditions [43], reached much the same conclusion but more fully addressed the effects of scene confusion factors on the expected retrieval accuracy using a very simple "blind" algorithm dependent only upon range. These results are summarized as follows (Fig. 11):

- 1) retrieval accuracy is optimized when radar resolution is smaller than the expected field-size dimensions of agricultural fields,
- 2) retrieval accuracy is optimized when radar resolution is coarser than local topographic variation in hilly areas,
- 3) the effects of row direction on retrieval accuracy are small, provided that the orbital trajectory yields azimuth view angles not orthogonal to row direction, and

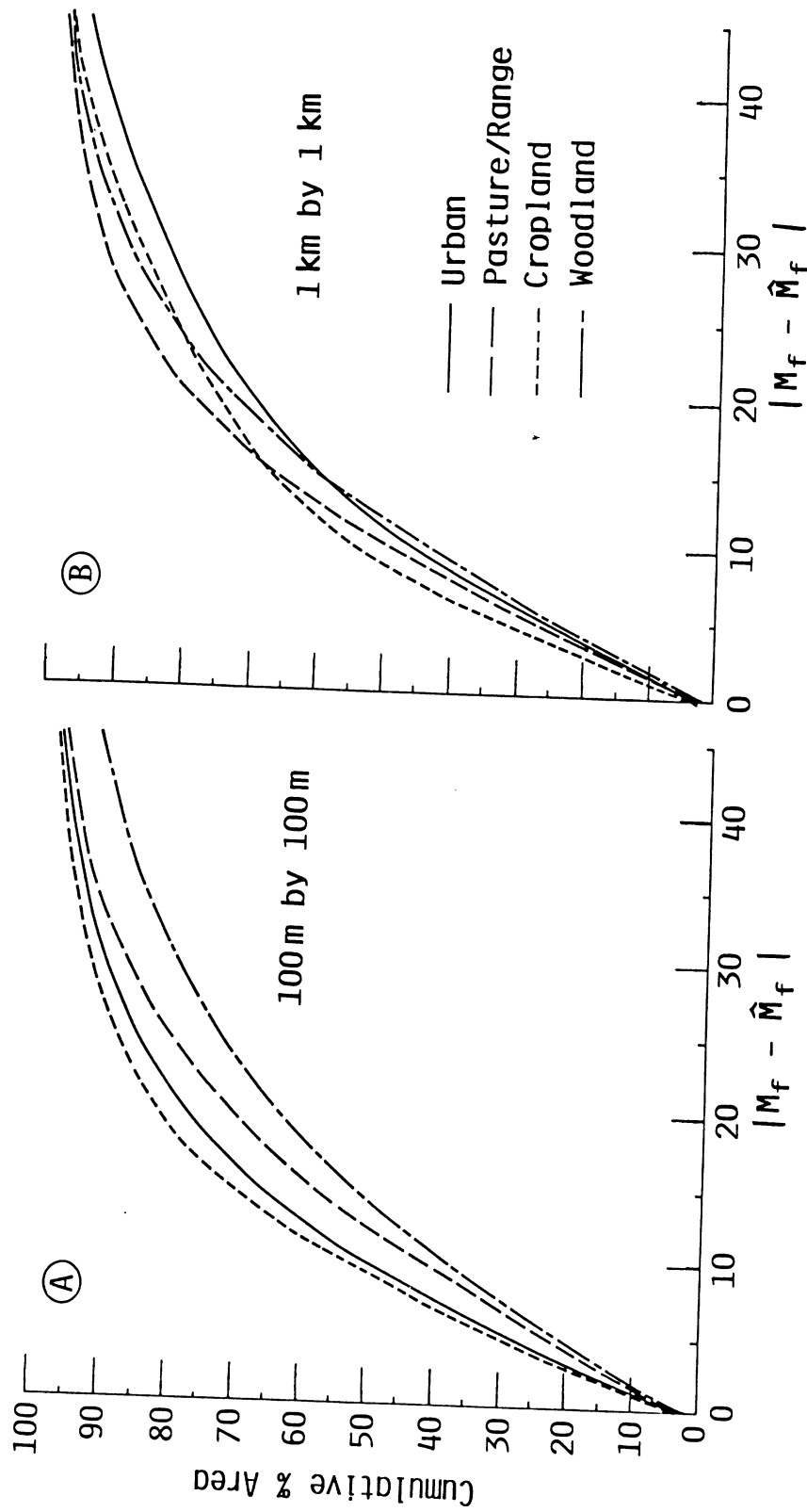


Figure 11. Cumulative percent area of all moisture-dependent pixels (excludes cultural features, water, and woodland) in each subregion as a function of absolute moisture classification error for (a) 100 m x 100 m radar resolution and (b) 1 km x 1 km radar resolution. M_f represents the true moisture and \hat{M}_f the moisture estimated by the radar (from [42]).

- 4) retrieval accuracy can be improved by about 10% when multidate change detection is used to provide updates.

The rationale for the postulated effectiveness of multidate change detection is based upon a simple consideration of scene-confusion factors and scene dynamics. For practical purposes, topography is constant, surface roughness decays slowly with time (except at critical points in the local crop calendar such as planting and harvest periods), and the interfield variance in canopy cover varies over periods of weeks for most canopies.

A change-detection approach applied to Seasat imagery over a test site in southwestern Kansas shows the technique to be effective for discriminating fields subjected to irrigation or tillage operations from larger spatial scale variations related to antecedent rainfall events [44]. The use of spatial filtering techniques on multidate "difference" images permits the ready distinction of these two general types of scene dynamics.

6.0 CONCLUSIONS

During the period of the AgRISTARS program, significant progress was made toward understanding the fundamental processes of target/sensor interaction, quantifying the effects of bulk scene properties and air-soil boundary conditions, developing both empirical and theoretical backscattering and emission models, and evaluating the potential performance of "optimal" orbital radar in terms both of sensor requirements and of possible soil-moisture retrieval methodologies. The research to date indicates that estimates of soil moisture in the 0 to 5 cm layer can be retrieved with reasonable accuracy for most requirements over agricultural areas from multirate and single-sensor observations. Such a system should operate at C-band over angles of incidence from about 10° to 20°. There is strong--but not conclusive--evidence to indicate that HV polarization will yield superior performance to HH polarization for soil-moisture retrieval.

There are, however, many pieces of the puzzle remaining to be fitted by means of further experimental investigation. For example, the precise physical role of soil texture as related to volumetric water content and soil matric potential with respect to radar backscattering is undefined at present. The utility of high-quality, cross-polarized backscattering in minimizing the effects of surface boundary conditions (i.e., topographic slope, small-scale roughness, and row direction) needs to be examined. The theoretical backscattering models must be rigorously tested

using data sets that provide sufficient physical characterization of the dielectric and roughness properties of soil. The effects of complex vegetation canopies on radar backscattering are only marginally understood and need further study. Finally, the confusion effects of complex geographical distributions of land-cover categories need to be better defined on the basis of the analysis of calibrated imagery.

REFERENCES

- [1] Schmugge, T. J., P. E. O'Neill, and J. R. Wang (1985), "Passive Microwave Soil Moisture Research," IEEE Trans. Geosci. Remote Sensing, GE-23, this issue.
- [2] Ulaby, F. T. (1974), "Radar Measurements of Soil Moisture Content," IEEE Trans. Antennas and Propag., AP-22, pp. 257-265.
- [3] Ulaby, F. T., J. Cihlar, and R. K. Moore (1974), "Active Microwave Measurement of Soil Water Content," Remote Sensing of Environment, 3, pp. 185-203.
- [4] Ulaby, F. T., and P. P. Batlivala (1976), "Optimum Radar Parameters for Mapping Soil Moisture," IEEE Trans. Geosci. Electronics, GE-14, pp. 81-93.
- [5] Ulaby, F. T., P. P. Batlivala, and M. C. Dobson (1978), "Microwave Backscatter Dependence on Surface Roughness, Soil Moisture, and Soil Texture: Part I--Bare Soil", IEEE Trans. Geosci. Electronics, GE-16, pp. 286-295.
- [6] Dobson, M. C., and F. T. Ulaby (1981), "Microwave Backscatter Dependence on Surface Roughness, Soil Moisture, and Soil Texture: Part III--Soil Tension," IEEE Trans. Geosci. Remote Sensing, GE-19, pp. 51-61.
- [7] Wang, J. R., and T. J. Schmugge (1980), "An Empirical Model for the Complex Dielectric Permittivity of Soil as a Function of Water Content," IEEE Trans. Geosci. Remote Sensing, GE-18, pp. 288-295.
- [8] Hallikainen, M., F. T. Ulaby, M. C. Dobson, M. El-Rayes, and L. K. Wu, (1985), "Microwave Dielectric Behavior of Wet Soil, Part I: Empirical Models and Experimental Observations," IEEE Trans. Geosci. Remote Sensing, GE-23, pp. 25-34.
- [9] Dobson, M. C., F. T. Ulaby, M. T. Hallikainen, and M. A. El-Rayes (1985), "Microwave Dielectric Behavior of Wet Soil, Part II: Dielectric Mixing Models," IEEE Trans. Geosci. Remote Sensing, GE-23, pp. 35-46.
- [10] Dobson, M. C., F. Kouyate, and F. T. Ulaby (1984), "A Reexamination of Soil Textural Effects on Microwave Emission and Backscattering," IEEE Trans. Geosci. Remote Sensing, GE-22, pp. 530-535.
- [11] Ulaby, F. T., and R. P. Jedlicka (1984), "Microwave Dielectric Properties of Plant Materials," IEEE Trans. Geosci. Remote Sensing, GE-22, pp. 406-414.

- [12] Ulaby, F. T., C. T. Allen, and A. K. Fung (1983), "Method for Retrieving the True Backscattering Coefficient from Measurements with a Real Antenna," IEEE Trans. Geosci. Remote Sensing, GE-21, pp. 308-313.
- [13] Schmugge, T. J. (1980), "Effect of Texture on Microwave Emission from Soils," IEEE Trans. Geosci. Remote Sensing, GE-18, pp. 353-361.
- [14] Bernard, R., Ph. Martin, J. L. Thony, M. Vauclin, and D. Vidal-Madjar (1982), "C-Band Radar for Determining Surface Soil Moisture," Remote Sensing of Environment, 12, pp. 189-200.
- [15] Wang, J. R. (1983), "Passive Microwave Sensing of Soil Moisture Content: Soil Bulk Density and Surface Roughness," Remote Sensing of Environments, Vol. 13, No. 4, pp. 329-344.
- [16] Waite, W. P., A. M. Sadeghi, and H. D. Scott (1984), "Microwave Bistatic Reflectivity Dependence on the Moisture Content and Matric Potential of Bare Soil," IEEE Trans. Geosci. Remote Sensing, GE-22, pp. 394-405.
- [17] Allen, C. T., F. T. Ulaby, and A. K. Fung (1982), "A Model for the Radar Backscattering Coefficient of Bare Soil," AgRISTARS SM-K1-04181, Remote Sensing Laboratory, University of Kansas Center for Research, Lawrence, KS.
- [18] Wilheit, T. T., Jr. (1978), "Radiative Transfer in a Plane Stratified Dielectric," IEEE Trans. Geosci. Electronics, GE-16, pp. 138-143.
- [19] LeToan, T., and M. Pausader (1981), "Active Microwave Signatures of Soil and Vegetation-Covered Surfaces. Results of Measurement Programs," Proc. ISP Int. Colloq. Spectral Signatures of Objects in Remote Sensing, Avignon, France, 8-11 September, pp. 303-314.
- [20] Hirosawa, H., S. Komiyama, and Y. Matsuzaka (1978), "Cross-Polarized Radar Backscatter from Moist Soil," Remote Sensing of Environment, 7, pp. 211-217.
- [21] Bradley, G. A., and F. T. Ulaby (1981), "Aircraft Radar Response to Soil Moisture," Remote Sensing of Environment, 11, pp. 419-438.
- [22] Jackson, T. J., A. Chang, and T. J. Schmugge (1981), "Aircraft Active Microwave Measurements for Estimating Soil Moisture," Photogram. Eng. Remote Sensing, 47, pp. 801-805.
- [23] Dobson, M. C., H. J. Eom, F. T. Ulaby, and A. K. Fung (1984), "Active and Passive Microwave Sensitivity to

- Near-Surface Soil Moisture and Field Flooding Conditions," Microwave Signatures in Remote Sensing (URSI Commission F), Toulouse, France, January 16-20, 1984.
- [24] Fung, A. K., and H. J. Eom (1983), "Coherent Scattering of a Spherical Wave from an Irregular Surface," IEEE Trans. Antennas Propag., AP-31, pp. 68-72.
- [25] Ulaby, F. T., R. K. Moore, and A. K. Fung (1985), Microwave Remote Sensing: Active and Passive, Vol. III, Dedham, MA: Artech House (forthcoming).
- [26] Ulaby, F. T., and J. E. Bare (1979), "Look-Direction Modulation Function of the Radar Backscattering Coefficient of Agricultural Fields," Photogram. Eng. Remote Sensing, 45, pp. 1495-1506.
- [27] Ulaby, F. T., F. Kouyate, A. K. Fung, and A. J. Sieber (1982), "Backscattering Model for a Randomly Perturbed Periodic Surface," IEEE Trans. Geosci. Remote Sensing, GE-20, pp. 518-528.
- [28] Blanchard, A. J., and A. T. C. Chang (1983), "Estimation of Soil Moisture from Seasat SAR Data," Water Resources Bull., 19, pp. 803-810.
- [29] Bush, T. F., and F. T. Ulaby (1978), "An Evaluation of Radar as a Crop Classifier," Remote Sensing of Environment, 7, pp. 15-36.
- [30] Attema, E.A.W., and F. T. Ulaby (1978), "Vegetation Modeled as a Water Cloud," Radio Science, 13, pp. 357-364.
- [31] Ulaby, F. T., C. T. Allen, G. Eger III, and E. Kanemasu (1984), "Relating the Microwave Backscattering Coefficient to Leaf Area Index," Remote Sensing of Environment, 14, pp. 113-133.
- [32] Eom, H. J., and A. K. Fung (1984), "A Scatter Model for Vegetation up to Ku-Band," Remote Sensing of Environment, 15, pp. 185-200.
- [33] Lang, R. H., and J. S. Sidhu (1983), "Electromagnetic Backscattering From a Layer of Vegetation: A Discrete Approach," IEEE Trans. Geosci. Remote Sensing, Vol. GE-21, No. 1, pp. 62-71.
- [34] Mo, T., T. J. Schmugge, and T. J. Jackson (1984), "Calculations of Radar Backscattering Coefficient of Vegetation-Covered Soils," Remote Sensing of Environment, 15, pp. 119-133.
- [35] Ulaby, F. T., A. Aslam, and M. C. Dobson (1982), "Effects of Vegetation Cover on the Radar Sensitivity to Soil Moisture," IEEE Trans. Geosci. Remote Sensing, GE-20, pp. 476-481.

- [36] Ulaby, F. T., and E. A. Wilson, "Microwave Attenuation Properties of Vegetation Canopies," IEEE Trans. Geosci. Remote Sensing, GE-23, this issue.
- [37] Allen, C. T., and F. T. Ulaby (1984), "Modeling the Polarization Dependence of the Attenuation in Vegetation Canopies," 1984 IEEE Int. Geosci. Remote Sensing Symp. (IGARSS'84) Digest, Strasbourg, France, 27-30 August.
- [38] Brunfeldt, D. R., and F. T. Ulaby (1984), "Measured Microwave Emission and Scattering in Vegetation Canopies," 1983 IEEE Int. Geosci. Remote Sensing Symp. (IGARSS'83) Digest, Vol. II, San Francisco, CA, 31 August - 2 Sept. (IEEE Cat. No. 83CH1837-4).
- [39] Ulaby, F. T., G. A. Bradley, and M. C. Dobson (1979), "Microwave Backscatter Dependence on Surface Roughness, Soil Moisture, and Soil Texture, Part II: Vegetation-Covered Soil," IEEE Trans. Geosci. Remote Sensing, GE-17, pp. 33-40.
- [40] Ulaby, F. T., B. Brisco, and M. C. Dobson (1983), "Improved Spatial Mapping of Rainfall Events with Spaceborne SAR Imagery," IEEE Trans. Geosci. Remote Sensing Let., GE-21, pp. 118-122.
- [41] Ulaby, F. T., M. C. Dobson, J. Stiles, R. K. Moore, and J. C. Holtzman (1982), "A Simulation Study of Soil Moisture Estimation by a Space SAR," Photogram. Eng. Remote Sensing, 48, pp. 6545-6560.
- [42] Dobson, M. C., F. T. Ulaby, and S. Moezzi (1982), "Assessment of Radar Resolution Requirements for Soil Moisture Estimation from Simulated Satellite Imagery," RSL Tech. Rep. 551-2, Remote Sensing Laboratory, University of Kansas Center for Research, Lawrence, KS.
- [43] Dobson, M. C., S. Moezzi, F. T. Ulaby, and E. Roth (1983), "A Simulation Study of Scene Confusion Factors in Sensing Soil Moisture from Orbital Radar," RSL Tech. Rep. 601-1, Remote Sensing Laboratory, University of Kansas Center for Research, Lawrence, KS.
- [44] Brisco, B., F. T. Ulaby, and M. C. Dobson (1983), "Spaceborne SAR Data for Land-Cover Classification and Change Detection," 1983 IEEE Int. Geosci. Remote Sensing Symp. (IGARSS'83) Digest, San Francisco, CA, 31 August - 2 Sept. (IEEE Cat. No. 83CH1837-4).